AIR FORCE INSTITUTE OF TECHNOLOGY

AIR UNIVERSITY
UNITED STATES AIR FORCE

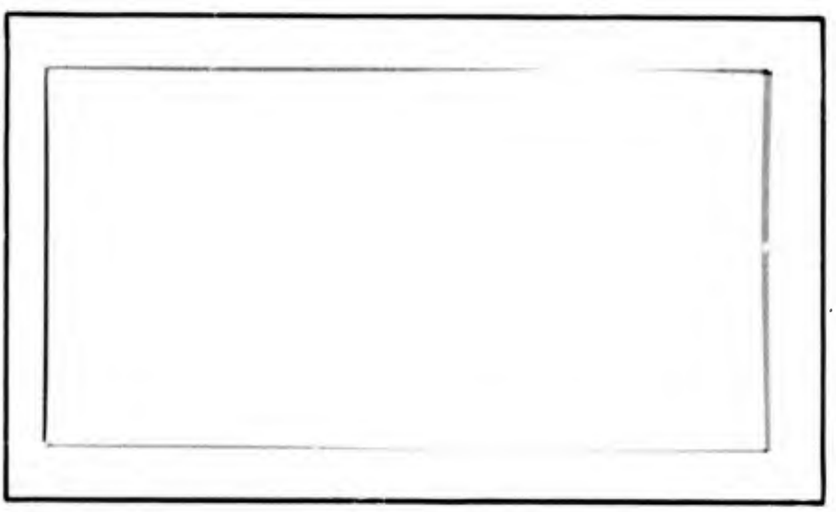

SCHOOL OF ENGINEERING

WRIGHT-PATTERSON AIR FORCE BASE, OHIO

AN EXPERIMENTAL STUDY OF MOLIERE'S THEORY OF MULTIPLE SCATTERING

THESIS

Earl L. Meurer
1/Lt. USAF
GA/Phys/69-4

AFLC-WPAFB-JUL 69 35

BLANK PAGE

AN EXPERIMENTAL STUDY OF MOLIERE'S THEORY OF MULTIPLE SCATTERING

THESIS

Presented to the Faculty of the School of Engineering of
the Air Force Institute of Technology
Air University
in Partial Fulfillment of the
Requirements for the Degree of
Master of Science

by

Earl L. Meurer, B.S.
1/Lt. USAF
Graduate Astronautics

June 1969

Preface

The following text is a report of the small angle multiple scattering study which I have been conducting for the past year. In this report, I have attempted to maintain a systematic development in presenting the experimental approach used and the results obtained in this study.

I would like to express my appreciation to CWO James T. Miskimen, head of the AFIT Physics Laboratory, for his sound advice throughout this study. Also, to Mr. Ron Gabriel who offered so freely of his time to help me eliminate equipment problems and to Mr. Earl D. Vance who did the machine work necessary for the modifications to the scattering apparatus. I am most grateful to Lt. Col. Ed Battle, a dedicated and patient instructor whose outstanding instruction resulted in the success I have had in this project.

Contents

Contents

List of Figures

List of Tables

List of Symbols and Abbreviations

Roman Letters

a	shielding distance
b	impact parameter
B	variable introduced in Moliere's theory for notational convenience
C	a constant
e	base of Naperian logarithms
e, q	electronic charge
e_o	permittivity constant
E, E_o	electron beam energy
f	beam particle distribution function
f^o, f^1 and f^2	terms in the series expansion of $f(\phi,Z)$
$f(\theta,Z)$	the number of beam particles scattered into a unit angle centered about θ, after traveling a distance Z into the plasma
$f(\phi,Z)$	the number of beam particles scattered into a unit angle centered about ϕ, after traveling a distance Z into the plasma
F_{ext}	external force applied to a system
i	index notation
I	attenuated beam current
I	normalized plasma-on survival current
I_{cold}	normalized plasma-off detector current
I_d	detector current
I_{hot}	normalized plasma-on detector current neglecting plasma scattering
I_i, I_o	input beam current
I_o	normalized plasma-off survival current

I_p	profile current measured by small cup
I_1, I_2	non-dimensional detector current at the number densities N_1 and N_2, respectively
K	temperature - degree Kelvin
k	$\times 10^3$
L	distance of the detection cup from the interaction chamber
m	particle mass
N	number density
N_1, N_2	number densities at two arbitrary neutral gas pressures
P	pressure
r	distance from beam center line (and perpendicular to)
r	incident particle distance from the target center
r_d	detector cup radius
r_m	minimum distance of incident particle from the target center
S	total scattering cross-section
t	time
T	temperature
v	volt (ev - electron volt)
$\bar{v}$	vector notation for the velocity space components v_x, v_y and v_z
w	solid angle
x, Z	penetration distance of a beam particle through a homogeneous gas or plasma
x, Z	interaction distance
X	scattering angle for a single collision in the multiple scattering concept
Z_e	net charge of a scattering particle

Greek Letters

α	angle defined in Fig. 2-1
α_m	value of α corresponding to r_m
β	deflection angle of a beam particle after a collision
γ_a	screening angle
γ_c	critical angle
δr	incremental change of radius r
θ	non-dimensional Moliere angle
θ_d	non-dimensional Moliere angle for detector cup
λ_d	Debye length, also plasma Debye length
λ_{d_e}	electron Debye length
λ_{d_i}	ion Debye length
π	3.1416
$\sigma(w)$	differential scattering cross-section as a function of the angle w
$\sigma(X)$	differential scattering cross-section as a function of the angle X
$\sigma(\beta)$	differential scattering cross-section as a function of the angle β
ϕ	particle deflection angle
ϕ	cumulative angle of scatter of the beam
ϕ'	direction of the electrons prior to being scattered into the angle ϕ
ϕ_1, ϕ_2	arbitrary values of ϕ
$\phi(r)$	potential field function
ϕ_d	detector size

Abstract

Electron beam scattering techniques using a single scattering theory can be used to determine the charged particle number density in a plasma. In this work, the possible use of electron beam scattering in the multiple scattering regime' was investigated.

A small angle scattering device, constructed in a previous thesis program, was modified to give better resolution and semi-automated data retrieval. Additional modifications to improve electron gun life and Langmuir probe measurements significantly improved the apparatus. In regards to the multiple scattering theory used, it has now been rather clearly indicated by Case and Battle that the Moliere theory of multiple scattering developed for electron scattering in thick foils is also the proper description for the present process.

The solution to the problem was found by experimentally measuring the electron beam current attenuation through a plasma and determining the plasma charged particle number density independently using a Langmuir probe. The attenuated beam current was then compared to that predicted by Moliere's theory for the same number density. From this, it was concluded that electron beam scattering techniques using Moliere's theory of multiple scattering could indeed be used to imply charged particle number density in a plasma.

BLANK PAGE

I. Introduction

The ionosphere and stellar bodies are examples of plasmas in nature, while man-made plasmas can be found in jet engine exhausts, energy converters, and many other applications. As the engineering and science fields become more advanced, there will undoubtedly be more areas where plasmas play a central role. Thus, the study of plasma dynamics becomes necessary to enable man to better understand, as well as to improve, his invironment.

One of the best known diagnostic tools available for plasma studies is the Langmuir probe, from which can be inferred the ion and electron number densities of a plasma. The interpretation of the data becomes questionable in highly non-equilibrium plasmas and in flows perturbed by the probe itself. As a result of work done at the University of Toronto, electron beam scattering was considered as an alternative means of determining charged particle number densities. From a recent study by Battle, it was concluded that electron beam scattering techniques could indeed be used to infer charged particle number densities (Ref. 1).

The terms "beam" and "plasma" carry several meanings in the scientific community, however, for this report, the term "beam" will imply a medium energy electron beam (0.5 to 2.5 kev), and the term "plasma" will imply a weakly ionized gas (ionization fraction $\approx 10^{-5}$) such as that used in common laboratory plasma experiments.

The scattering of particles from an electron beam can be accomplished in two ways. The first is "single scattering" in which a beam particle is deflected from the beam by a charged or neutral

particle and lost forever. Any subsequent collisions only serve to deflect the particle further from the beam. This approach is common in neutral and very weak plasma studies. The second is "multiple scattering" where beam particles can be lost from the beam, over and above that due to single scattering, by a large number of small angle deflections.

Several theories have been published which predict the distribution of the beam particles after passing through the plasma (Ref. 6, 9, 11 and 13). Among these is "Moliere's Theory of Multiple Scattering." This theory has been found to be ideally suited for plasma studies because of the few restrictions or assumptions made in the scattering problem. Another desirable feature is its applicability to both the single and the multiple scattering problem.

Thus, the Moliere theory was used in this project, the multiple scattering study previously suggested by Battle. The purpose of this report is to describe the procedures used and the results and conclusions obtained from this study.

To obtain experimental data, the small angle scattering device constructed by Wawak for laboratory use (Ref. 16) was modified to provide semi-automatic data retrieval and improved angular resolution. When completed, a preliminary single scattering study, briefly considered by Wawak, was conducted using argon gas.

Having eliminated as much procedural and equipment errors as possible, the multiple scattering investigation began. Bethe's solution to Moliere's theory was programed and outputs obtained for expected operating conditions. Again using argon gas, experimental multiple scattering measurements were made using the small angle

scattering device. Charged particle (or scatterer) number densities were determined independently, from Langmuir probe measurements. The measured multiple scattering in the plasma for the calculated total charged particle number density, ion plus electron, was then compared to the scattering predicted by Moliere for the same scatterer number density. This comparison was the measure used to determine whether charged particle number density can be determined from electron beam techniques, using the Moliere theory.

This report will be limited to presenting some basic single collision theory as a foundation for the more difficult multiple collision concept. Bethe's solution to the Moliere theory will then be presented and used to predict the multiple scattering which will occur for given experimental conditions. The experiments will be discussed and their results compared to theory. A discussion of observations, conclusions and recommendations will also be included.

II. Theoretical Considerations

Neutral Scattering

The fundamental theoretical equations governing basic scattering processes are well established and can be found in any elementary plasma diagnostics text (Ref. 10 & 12). In addition, Wawak discusses these equations and their application to the small angle scattering device used in this study as well as considerations to be made when applying them. Rather than repeat his work, this section will be devoted to giving a brief summary of the equations applicable to the single scattering experiment as an introduction to the more difficult multiple scattering experiment.

The attenuation which occurs when an electron beam of initial intensity I_o passes a distance x through a homogeneous gas is given by

$$\frac{I}{I_o} = e^{-SNx} \tag{1}$$

(Ref. 1:3)

where S is the total scattering cross-section in dimensions of area and N is the scatterer number density in particles per unit volume. Extensive theoretical work has been done to predict S for given experimental conditions.

The defining equation for S is given by

$$S = \int\int \sigma(w)\, dw \tag{2}$$

where $\sigma(w)$ is the differential scattering cross-section and is defined as the number of particles per unit time scattered into a solid angle between w and (w + dw), per unit solid angle, per unit incident flux, by one scatterer. In terms of the angle defined in Fig. 2-1, this can

be written as:

$$S = 2\pi \int_{o}^{\pi} \sin\beta \; \sigma(\beta) d\beta \tag{3}$$

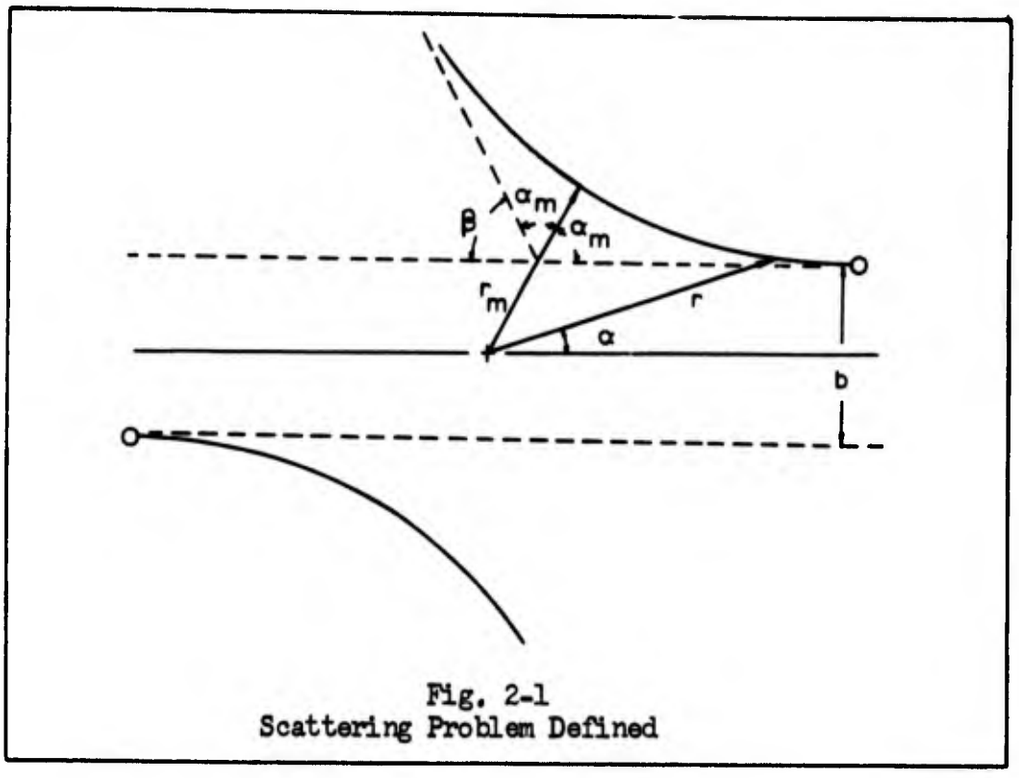

Fig. 2-1
Scattering Problem Defined

By using total energy and angular momentum relations with reference to Fig. 2-1, a new relationship is obtained:

$$\frac{dr}{d\alpha} = \frac{r^2}{b}\left[1 - \frac{b^2}{r^2} - \frac{\phi(r)}{E_o}\right]^{\frac{1}{2}} \tag{4}$$

(Ref. 7:117)

where $\phi(r)$ is the potential field of the target particle, E_o is the kinetic energy of the incident beam particle, r is the incident particle distance from the target center and b is the impact parameter. Thus, if the potential field function is repulsive, then the value of β is given by:

$$\beta = \pi - 2b\int_{r_m}^{\infty} \left[\frac{d\alpha}{dr}\right] dr \qquad (5)$$

(Ref. 7:117)

where r_m is the value of r for which $\dot{r} = 0$ and can be found from angular momentum considerations.

From conservation of particles, it can be shown that

$$\sigma(\beta) = \frac{b}{\sin \beta} \frac{db}{d\beta} \qquad (6)$$

(Ref. 7-116)

for three dimensional scattering.

Ideally then, the problem is solved. Inserting the exact form of $\phi(r)$ in Eq. (5) and integrating yields b as a function of β. Substituting this into Eq. (6) gives the differential scattering cross-section, $\sigma(\beta)$, which will give the total scattering cross-section when integrated over all β. However, for electron-neutral atom scattering the interaction potential is sometimes a complicated function requiring numerical techniques to solve for S. Several suitable approximate techniques have been developed for calculating this potential. One of these is the Thomas-Fermi, which may be approximately represented over portions of its range by a function of the form:

$$\phi(r) = \frac{Z_e C e^{-r/a}}{r/a} \qquad (7)$$

(Ref. 1:6)

where Z_e is the net charge of the scattering particle, a is the appropriate shielding distance and C is a constant. This is also the potential field for a charged particle in an equilibrium plasma when the shielding distance is interpreted as the plasma Debye length. The total scattering cross-sections calculated for neutral and charged

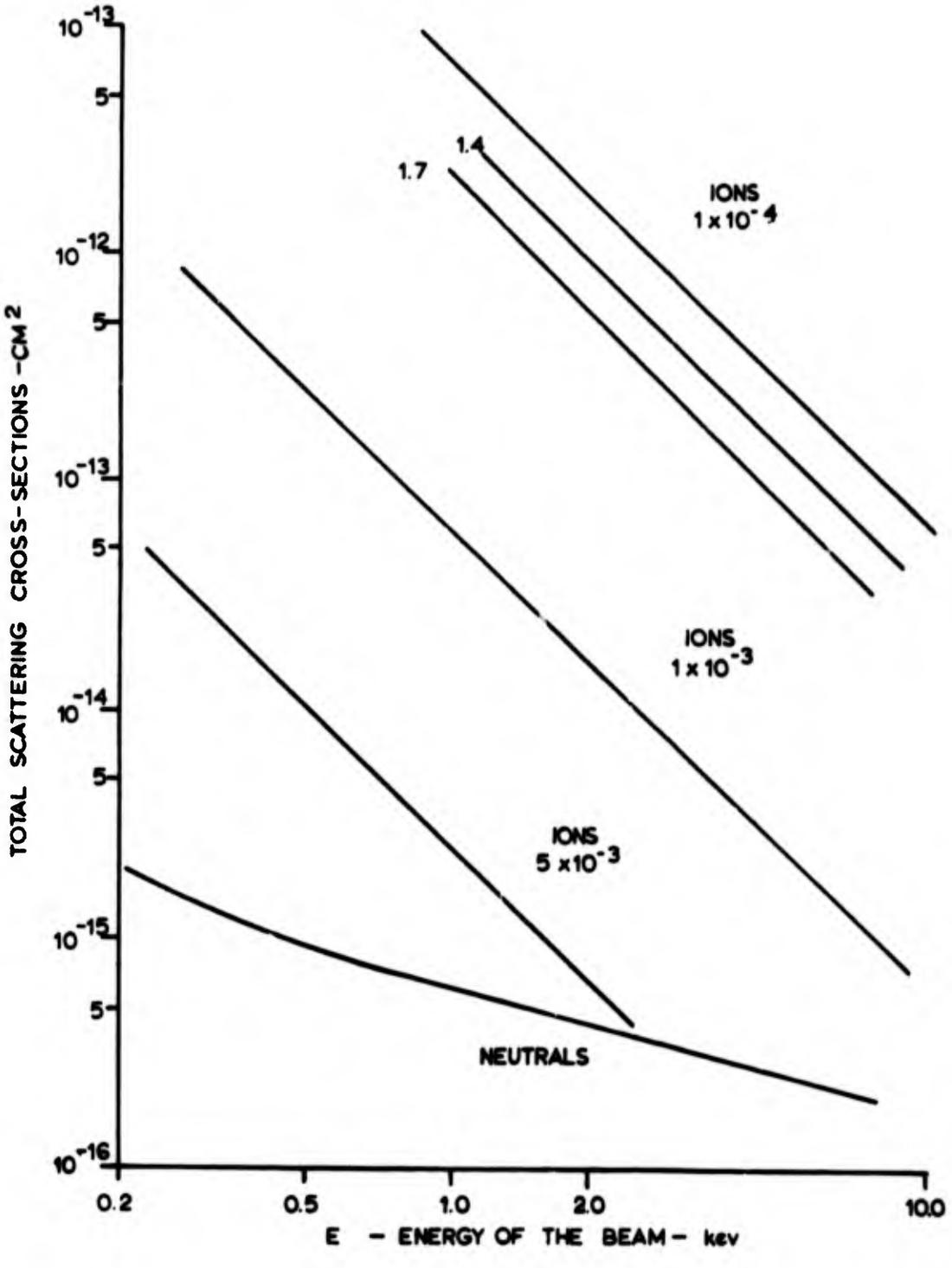

FIG. 2-2
TOTAL SCATTERING CROSS-SECTIONS
FOR ELECTRONS IMPINGING ON STATIONARY
ARGON ATOMS AND SINGLY CHARGED ION SCATTERING SPECIES

(REF. 1:61)

particle scattering using the numerical Thomas-Fermi potential and the screened Coulomb respectively are plotted against beam energy in Fig. 2-2 (from Ref. 1). It is interesting to note that only one curve is necessary for neutral scattering because the shielding distance is many orders smaller than the shielding distance for charged particle scattering. Therefore, over the small collector angle range covered in this figure there is no discernable variation in neutral scattering cross-section.

From these calculations, the neutral scattering cross-section is seen to be weakly dependent upon beam energy, while charged particle scattering cross-sections are shown to be highly sensitive to both detector angle and beam energy. If a simple approximation is used for the scattering potential, such as an inverse power law, scaling laws can be derived which show analytically this scaling (Ref. 10-73 and 7-117).

As a preliminary study, a neutral scattering experiment was conducted to determine the neutral scattering cross-sections for argon gas. In this experiment, the cross-sections were determined for different beam energies and detector sizes by plotting the logarithm of the current ratio I/I_o against the product of number density and interaction distance. The results of this study are discussed in Chapter IV.

Comments on the Single Scattering Approach

In this report, attention is restricted to small angle scattering ($\sin\beta \approx \beta$) of low energy electron beams (about 2 Kev) by weakly ionized plasmas. Thus, ions and electrons present the same cross-

section to an incoming electron beam particle (Ref. 1:8). For this reason, reference will be made only to charged particles and neutrals with the charged particle number density taken as the sum of the electron and ion number densities. The scattering particle distribution is assumed homogeneous in the theory, and all measurements of particle density will be assumed to be averages over the interaction length. Also, finite beam effects are neglected.

It should be noted that all collisions here have been assumed to be single scattering, that is, all beam particles are assumed to be lost on the first collision with any subsequent collisions only deflecting them further out. No beam particles are ever returned to the beam by a collision.

If the charged particle number density and interaction distance are increased enough, the total number of successive collisions becomes large and the particle can be lost by a succession of small angle collisions, each smaller than the detector angle. At this point, the problem becomes statistical and the resulting particle distribution can be shown to be Gaussian by using the central limit theorem (Ref. 3). This is multiple scattering.

Multiple (Plural) Scattering

Before complete transition from single to multiple scattering, there exists a region where many small angle collisions occur but these are not sufficient in number to allow a statistical theory. This region is defined as the plural scattering regime' and requires more sophisticated analysis. At least four different theories have been published on this subject which are mathematically closely

related and can give exact results if evaluated carefully (Ref. 6, 9, 11 and 13).

Of these, the Moliere Theory of Multiple Collisions (Ref. 11) is the most advantageous in that it is simplier than the others, completely independent of the form of the differential scattering law, and it remains analytic throughout. Originally, the Moliere theory was created to solve the problem of an electron beam penetrating a thick foil but it is valid for single, plural, and multiple plasma scattering.

In a later paper, by Bethe (Ref. 2), an alternative and more physical derivation of the governing equation is given as well as a more complete tabulation of its solution. The mechanics of both solutions have been worked out in detail and will not be repeated here. Moliere's theory will be discussed as it applies to the problem and Bethe's work will be used for computations.

This section will discuss only plural scattering with no further mention of statistical multiple scattering. Therefore all further references to multiple scattering will be understood to be the plural regime'.

Moliere Theory of Multiple Scattering

Although the Boltzmann equation is not exact for the case of long range forces between charged particles, attempts have been made to overcome the recognized limitations (Ref. 1-A8). As will be shown, Moliere follows this approach in using the basic Boltzmann equation as the foundation for his theory. Written in standard notation, the Boltzmann equation is:

$$\frac{\partial f(\phi,Z)}{\partial t} + \bar{v} \cdot \frac{\partial f(\phi,Z)}{\partial \bar{x}} + \frac{F_{ext}}{m} \cdot \frac{\partial f(\phi,Z)}{\partial \bar{v}} = \frac{\partial f(\phi,Z)}{\partial t}\Big]_{coll} \tag{8}$$

where $f(\phi,Z)$ is the number of beam particles scattered into a unit angle centered about ϕ, after traveling a distance Z into the plasma. Following the lead of others, Moliere assumed the collision term to consist of two parts:

$$\frac{\partial f(\phi,Z)}{\partial t} = -Nf(\phi,Z)\int\sigma(X)XdX + N\int f(\phi',Z)\sigma(X)dX \tag{9}$$

(Ref. 2:1257)

where N is the number of scattering particles, i.e., the total number of electrons plus ions per unit volume in the plasma; ϕ is the cumulative angle of scatter of the beam, ϕ' is the direction of the electrons prior to being scattered into the direction depicted by ϕ, and the angle X is the scattering angle for each single collision.

The first term in Eq. (9) is the familiar form for close encounters and the second is a diffusion term representing scattering back into the beam. Moliere's diffusion term differs from previous results in that it is a single exact equation which applies to all regions. However, several implicit assumptions are made: a) The angles are small compared to a radian, therefore $\sin\phi \approx \phi$; b) All collisions are sequentially occurring, two body types and therefore describable by a differential scattering cross-section; c) The electron beam is ideal; d) The beam is mono-energetic and the scatterers cold or appropriate averages over relative velocities are to be used for the cross-sections.

Before discussing the end results of Moliere's theory, the

features offered by this theory as outlined by Case and Battle (Ref. 4:201) are worth noting.

a) Perhaps the most important feature of Moliere's theory is that the scattering is described by a single parameter, the screening angle γ_a. The ratio of this angle, which describes the scattering particle, and the critical angle γ_c, which describes the plasma, determines the angular distribution. Thus the distribution function is independent of the form of the differential scattering cross-section provided only that it goes to the Rutherford law for large angles.

b) The cross-sections of the electrons and ions as seen by the beam are the same because of the small angle approximation.

c) For small angles, no energy is transferred in an elastic electron-electron collision, allowing use of a Dirac delta for the beam distribution function.

d) The functional form of the angular distribution of the scattered electrons $f(\phi,Z)$ will not depend on the charged particle number density.

From a physical viewpoint, the presence of a screening angle implies a potential function similar to the Thomas-Fermi. Using this potential function with the screening distance defined as the effective Debye length for the plasma,

$$\frac{1}{\lambda_d^2} = \frac{1}{\lambda_{d_e}^2} + \frac{1}{\lambda_{d_i}^2} \tag{10}$$

one can obtain an analytical solution for the screening angle

$$\gamma_a = \frac{q^2}{4\pi\epsilon_o E}\lambda_d \tag{11}$$

where q is the electron charge, e_o is the permittivity constant and E is the beam energy. It should be noted that the differential scattering cross-section enters the theory only through this screening angle.

The details of the solution to Moliere's theory can be found in Bethe's work. The results can be summarized in brief. A new variable B is introduced for notational convenience:

$$B - \ln B = \ln (\gamma_c/\gamma_a)^2 - 0.154 \tag{12}$$

(Ref. 4:202)

The value of B is usually between 5 and 20. Also, a non-dimensional angle θ is defined by:

$$\theta = \phi/B^{\frac{1}{2}}\gamma_c \tag{13}$$

Thus, knowing the screening angle and critical angle yields B from Eq. (12) which in turn gives θ for known real angle ϕ. This then yields the beam distribution from

$$f(\theta,Z) = \frac{1}{B\gamma_c^2}\left[f^o(\theta) + \frac{1}{B}f^1(\theta) + \frac{1}{B^2}f^2(\theta) + \cdots\right] \tag{14}$$

(Ref. 2:1259)

where f^o, f^1 and f^2 are the terms in a series expansion of $f(\phi,Z)$ and are tabulated by Bethe as shown in Table I. In his work, Bethe shows that truncating after the third term gives accuracy to about one per cent or better. The f^o term is the statistical multiple scattering solution (Gaussian) and at small angles, i.e., θ less than 2, this term is dominant. The 1/B factor on the f^1 term makes the correction only about 10 per cent at the small angles. At large angles, f^o goes to zero and the f^1 and f^2 terms are dominant.

The profile of the beam distribution after scattering can be

Table I

Bethe's Solution to Moliere Theory

θ	f^0	f^1	f^2
0.0	2.0	0.8456	2.4929
0.2	1.9216	0.7038	2.0694
0.4	1.7214	0.3437	1.0488
0.6	1.4094	-0.0777	-0.0044
0.8	1.0546	-0.3981	-0.6068
1.0	0.7338	-0.5285	-0.6359
1.2	0.4738	-0.4770	-0.3086
1.4	0.2817	-0.3183	0.0525
1.6	0.1546	-0.1396	0.2423
1.8	0.0783	-0.0006	0.2386
2.0	0.0366	+0.0782	0.1316
2.2	0.01581	0.1054	0.0196
2.4	0.00630	0.1008	-0.0467
2.6	0.00232	0.08262	-0.0649
2.8	0.00079	0.06247	-0.0546
3.0	0.000250	0.04550	-0.03568
3.2	$7x3x10^{-5}$	0.03288	-0.01923
3.4	$1.9x10^{-5}$	0.02402	-0.00847
3.6	$4.7x10^{-6}$	0.01791	-0.00264
3.8	$1.1x10^{-6}$	0.01366	0.00005
	$1000f^0$	$1000f^1$	$1000f^2$
4.0	$2.3x10^{-4}$	10.638	1.0741
4.5	$3x10^{-6}$	6.140	1.2294
5.0	$2x10^{-8}$	3.831	0.8326
5.5	$2x10^{-10}$	2.527	0.5368
6.0	$5x10^{-13}$	1.739	0.3495
7.0	$1x10^{-18}$	0.9080	0.1584
8.0	$3x10^{-25}$	0.5211	0.0783
9.0	$1x10^{-32}$	0.3208	0.0417
10.0	$1x10^{-40}$	0.2084	0.0237

obtained by selecting specific ϕ angles from zero to 180 degrees and plotting the resulting solutions of Eq. (12) versus their respective angle. From this distribution the current within any interval, say ϕ_1 and ϕ_2, can be calculated. From the definition of $f(\phi,Z)$, this can be determined from

$$I = \int_{\phi_2}^{\phi_1} f(\phi,Z)\phi d\phi \tag{15}$$

Theoretical Survival Current Calculation

From Eq. (15), the current measured by the input cup can be determined as

$$I_o = \int_o^{\pi} f(\phi,Z)\phi d\phi \tag{16}$$

Also, the current measured using a detector cup of size ϕ_d is

$$I = \int_o^{\phi_d} f(\phi,Z)\phi d\phi \tag{17}$$

where ϕ_d is the maximum angle at which beam particles can still be detected by the detector cup positioned along the beam center line. In Fig. 2-3, ϕ_d is defined in relation to r_d, the detector cup radius, and L, the distance of the detector cup from the interaction chamber.

The ratio of Eqs. (16) and (17) gives the non-dimensional survival current, a measure of the scattering occurring, and is written:

$$\frac{I}{I_o} = \frac{\int_o^{\phi_d} f(\phi,Z)\phi d\phi}{\int_o^{\pi} f(\phi,Z)\phi d\phi} \tag{18}$$

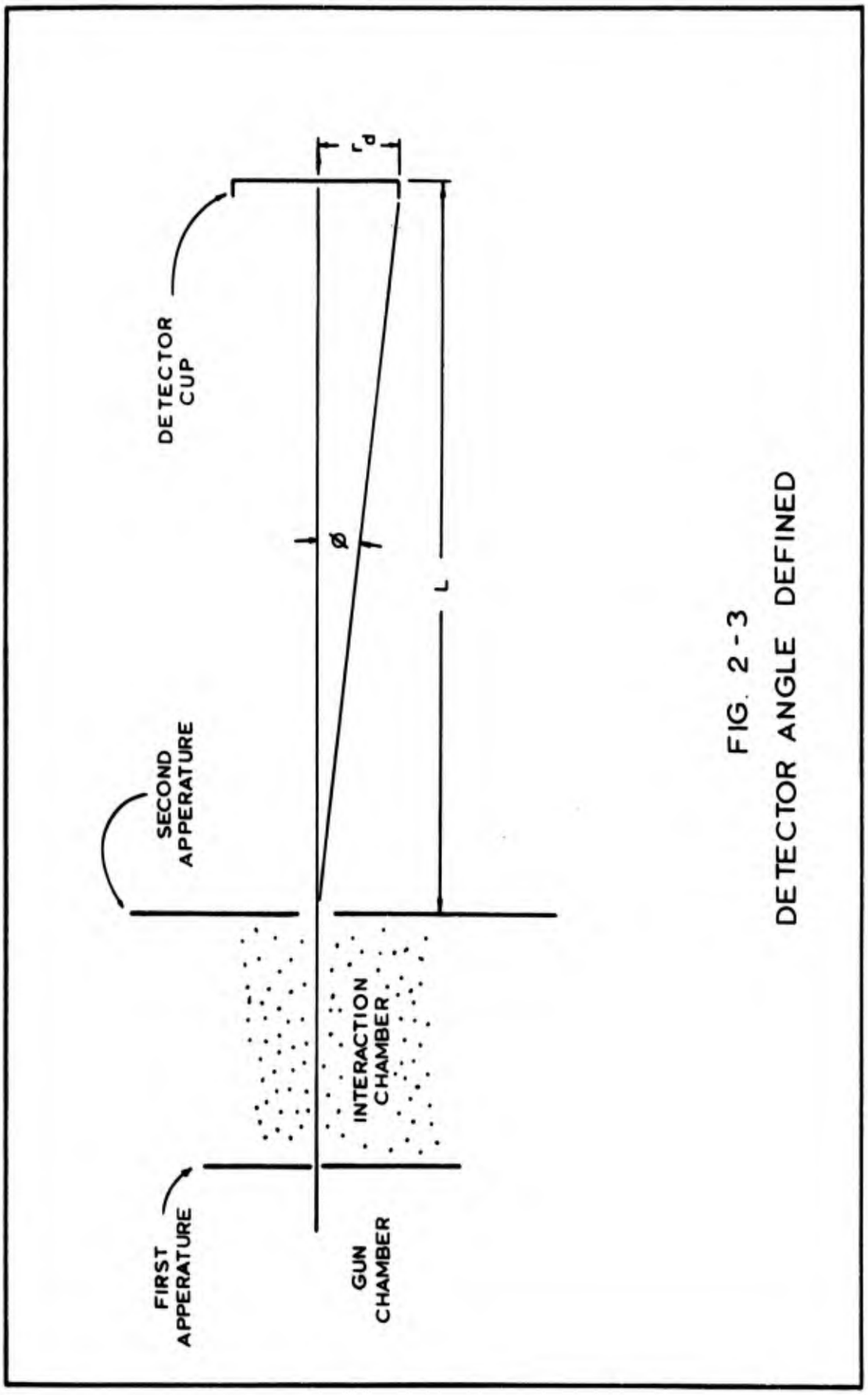

FIG. 2-3

DETECTOR ANGLE DEFINED

By rearranging, Eq. (18) can be written in terms of the non-dimensional angle θ defined by Eq. (13):

$$\frac{I}{I_o} = \frac{\int_o^{\theta_d} f(\phi,Z)\theta d\theta}{\int_o^{\pi} f(\phi,Z)\theta d\theta} \tag{19}$$

where $f(\phi,Z)$ is the number of beam particles scattered into a unit angle centered about ϕ, after traveling a distance Z into the plasma. Thus, this section will present the calculation procedure used to obtain the expected survival current for a set of fixed parameters.

From Eq. (12), a solution for B as a function of γ_c/γ_a was obtained. Since it can be shown that

$$\gamma_a/\gamma_c = 8.74 \times 10^{-4} \sqrt{E/ZT} \tag{20}$$

where E is the electron beam energy, Z is the interaction distance, and T is the plasma temperature, a graph of B as a function of ZT/E was constructed and is shown in Fig. 2-4. Knowing the system parameters Z, T and E, then B can be found easily.

Next, the value of the critical angle was determined using

$$\gamma_c^2 = \frac{Zq^2}{4\pi e_o^2} \frac{N}{E^2} \tag{21}$$

where q is the electron charge, e_o is the permittivity constant and N is the number density. For convenience in programing, this was rearranged into $\gamma_c^2 = CN/E^2$ where C is the constant given by:

$$C = \frac{Zq^2}{4\pi e_o^2} \tag{22}$$

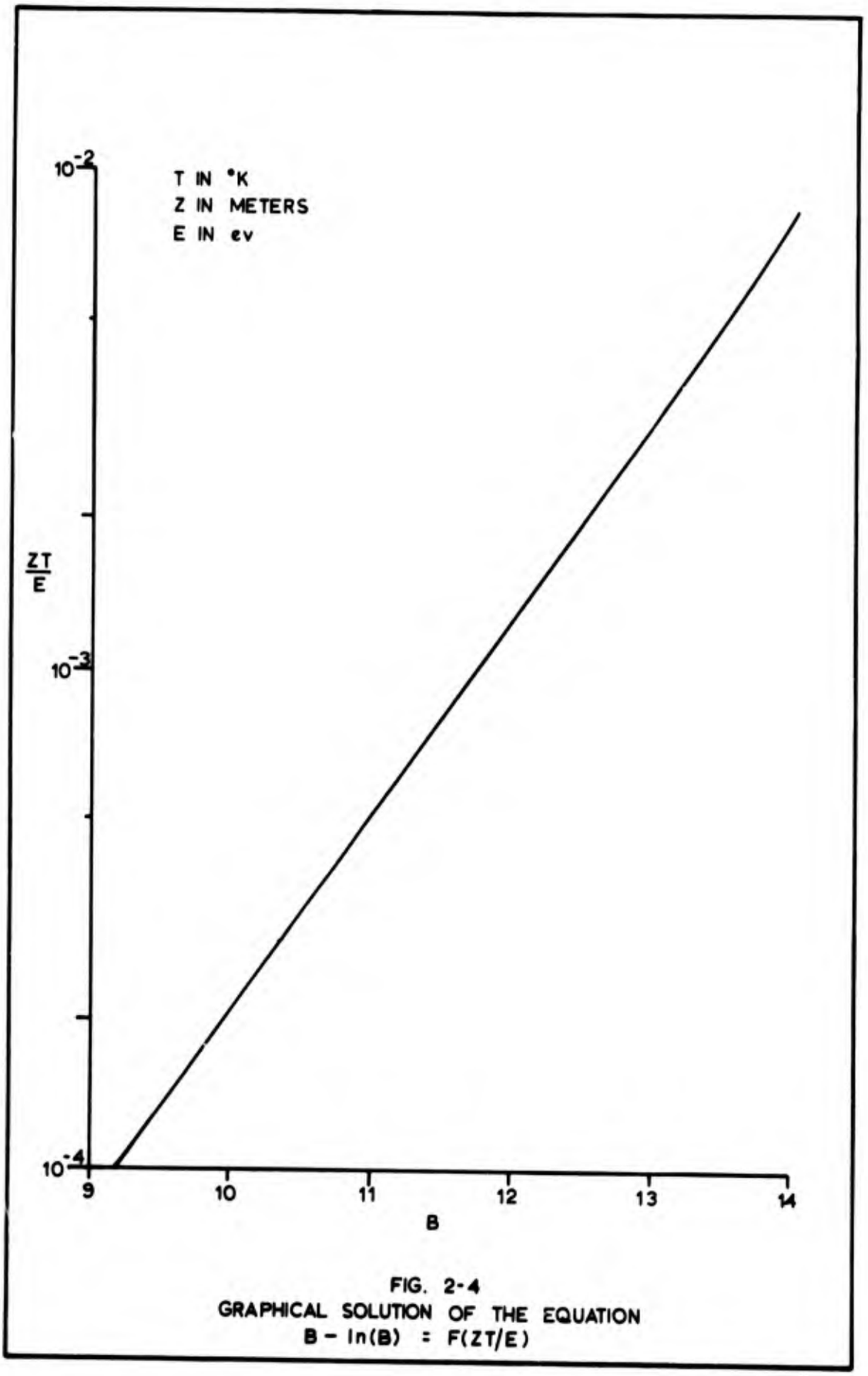

FIG. 2-4
GRAPHICAL SOLUTION OF THE EQUATION
$B - \ln(B) = F(ZT/E)$

Knowing B and γ_c for the given values of E, T, Z and N, then the non-dimensional value of ϕ_d, denoted by θ_d, can be calculated. After calculating θ_d, the value of $f(\phi,Z)$ at θ_d can be determined using the equation

$$f(\phi,Z) = \frac{1}{B\gamma_c^2}\left[f^o(\theta) + \frac{1}{B}f^1(\theta) + \frac{1}{B^2}f^2(\theta)\right] \qquad (23)$$

where f^o, f^1 and f^2 are tabulated in Table I. For values of θ not given in the table, the values of f^o, f^1 and f^2 can be found easily using the graphical representation of Bethe's solution shown in Figs. 2-5a and 2-5b. Note, however that $f(\phi,Z)$ yields only the beam particles scattered into the angle ϕ. The integration of $f(\phi,Z)$ over the cup apperature area will give the current measured by the cup.

To perform this integration numerically requires the value of $f(\phi,Z)$ to be computed for each interval chosen. That is, $f(0,Z)$, $f(0 + d\phi,Z)$, $f(0 + 2d\phi,Z)$ etc. Thus, the numerical integration equation can be written:

$$\frac{I}{I_o} = \frac{\sum_{o}^{\theta_d}(f_{i+1} + f_i)(\theta_{i+1} + \theta_i)(\theta_{i+1} - \theta_i)}{\sum_{o}^{\theta_{max}}(f_{i+1} + f_i)(\theta_{i+1} + \theta_i)(\theta_{i+1} - \theta_i)} \qquad (24)$$

the upper limit of the I_o integration was taken as a first approximation to be 10.

The entire technique was programed on an IBM 1620 computer and a set of expected parameters used in a sample calculation of the predicted survival currents. The parameters used were: beam energy -

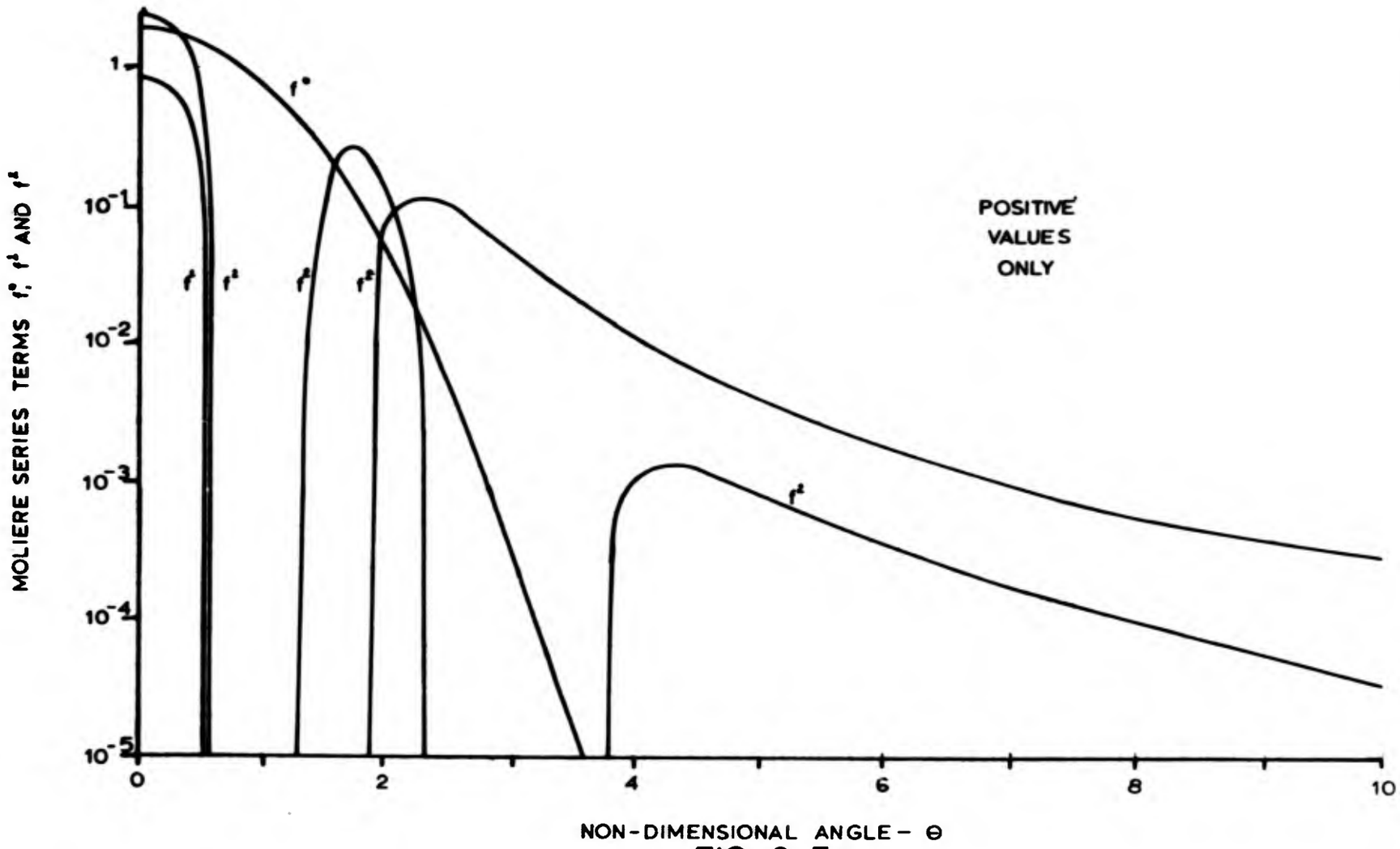

FIG. 2-5a

GRAPHICAL DISPLAY OF BETHE'S SOLUTION TO MOLIERE'S THEORY

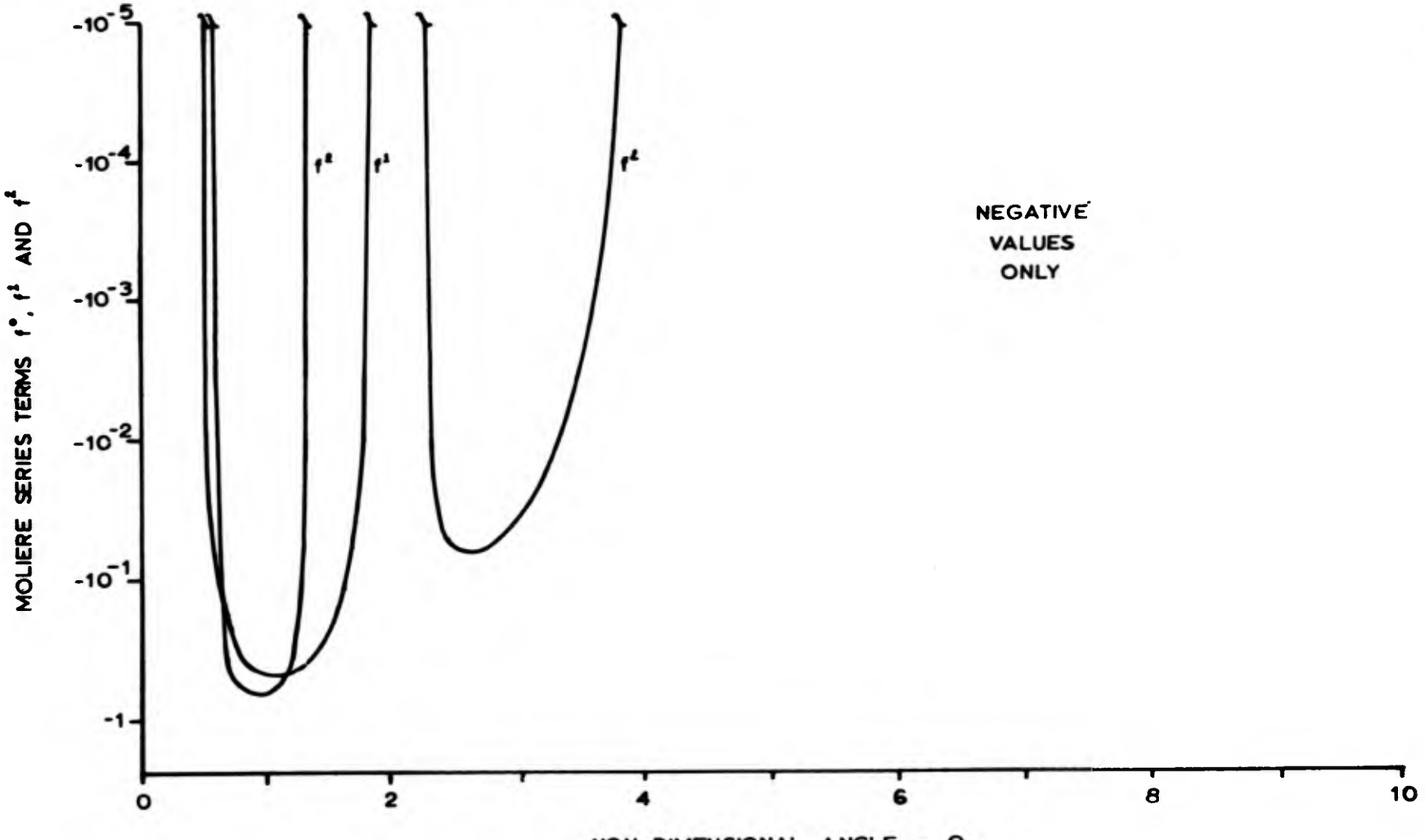

FIG. 2-5b

GRAPHICAL DISPLAY OF BETHE'S SOLUTION TO MOLIERE'S THEORY

1500 electron volts, interaction distance - 10 centimeters, plasma temperature - 298 degrees Kelvin, and ϕ_d - 2.0×10^{-4}. The results are shown in Fig. 2-6 for number densities in the range of 10^9 to 10^{12} per cubic centimeter and the program used is shown in Appendix C with the input data and results.

Fig. 2-6 shows, as expected, the predicted multiple scattering survival currents, shown by the heavy continuous line, to be much less than the single scattering theory predictions, shown by the beaded line. In addition to determining the predicted multiple scattering curve, it was of interest to know the effects of temperature, beam energy, and detector cup size. The dashed line shows predicted survival currents for a plasma temperature of 5000 degrees Kelvin. The greatest decrease in survival current is 15 per cent which is not unreasonable considering the magnitude of the temperature change.

The effects of beam energy and detector cup size are not shown. However, if either increases the curve shifts to the right. If increased enough, the Moliere curve joins the Rutherford curve and multiple scattering can no longer be detected.

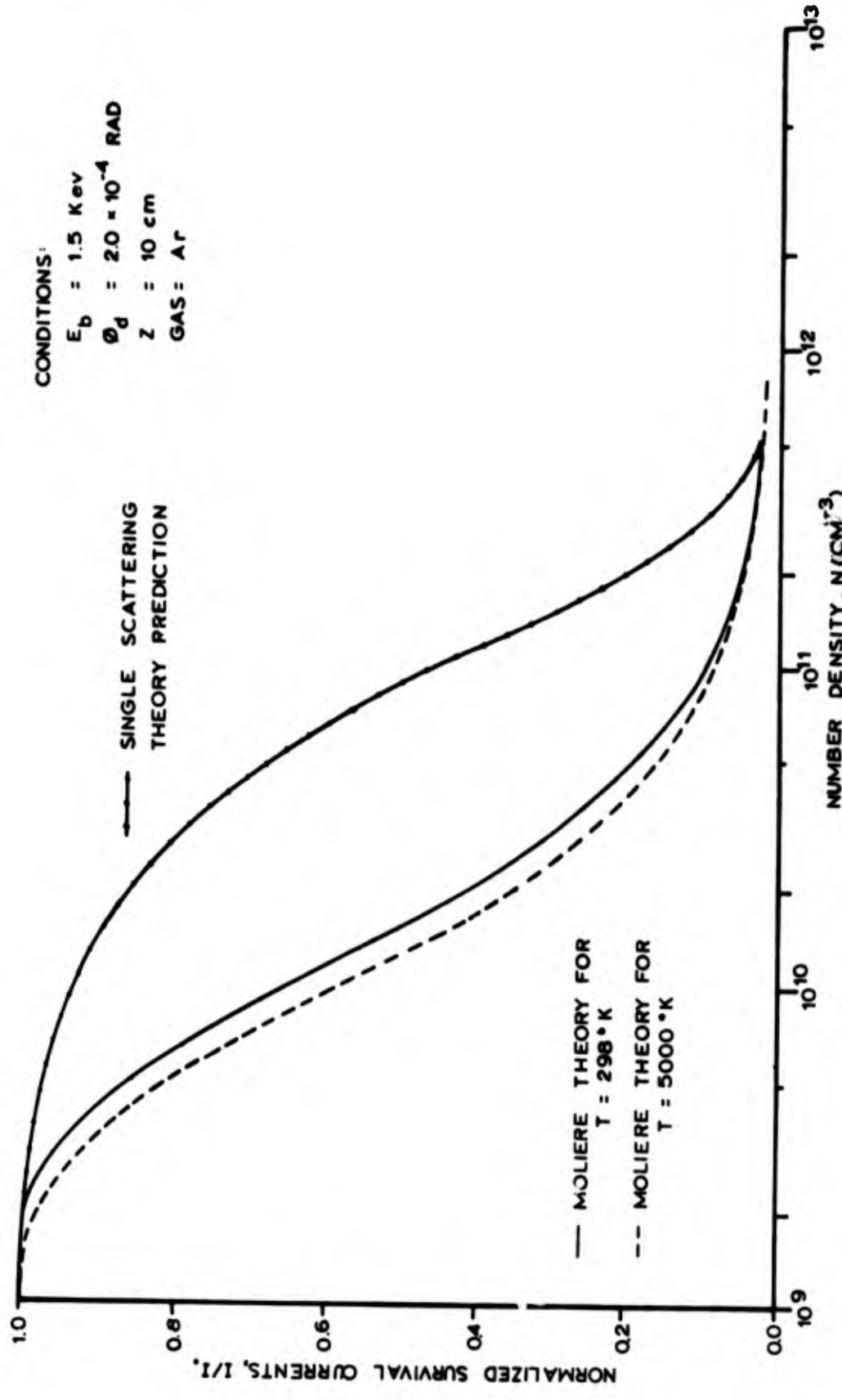

FIG. 2-6
MOLIERE AND RUTHERFORD
SURVIVAL CURRENT PREDICTIONS

III. Apparatus

The Basic Design

Since this thesis project is a continuation of the work of Wawak, the credit for construction of the apparatus used must go to him. Credit should also go to Battle whose original beam/interaction device served as the guide for the development of the present apparatus.

In his project, Wawak designed and built the small angle plasma/electron beam scattering device shown in Fig. 3-1 and conducted some preliminary tests. This same scattering device, with some modifications, was used in the single and multiple scattering experiments described in this report. In the interest of avoiding unnecessary repetition the reader is referred to Wawak's thesis for a detailed description of the device (Ref. 4). This section will be devoted instead to describing the modifications made to Wawak's equipment so that the goals of this thesis project could be accomplished. However, to acquaint the reader with the apparatus, a very brief description is presented first.

The basic design of the apparatus consisted of the scattering device and the necessary pumps, power supplies and measuring instruments. The scattering device, shown schematically in Fig. 3-2, was constructed of pyrex glass and had three separate sections; the gun chamber, the interaction chamber, and the detection chamber. The gun chamber, kept at a pressure of 10^{-8} torr by an oil diffusion pump, contained the electron gun which was held in place by an adjustable bellows mount. A low energy electron beam was formed in the gun chamber and columnated by a one millimeter apperature as it passed

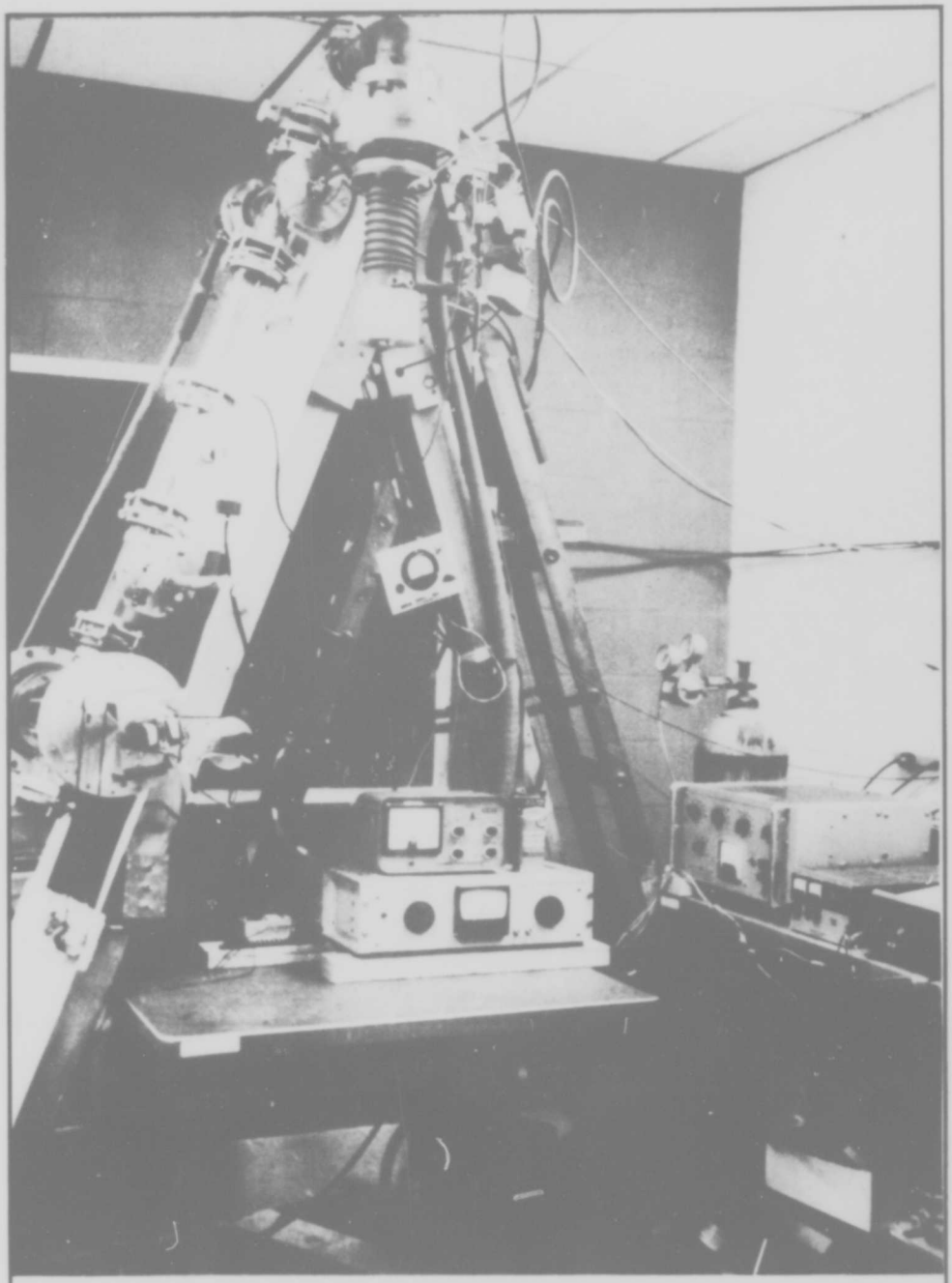

FIG. 3-1
THE SMALL ANGLE SCATTERING DEVICE

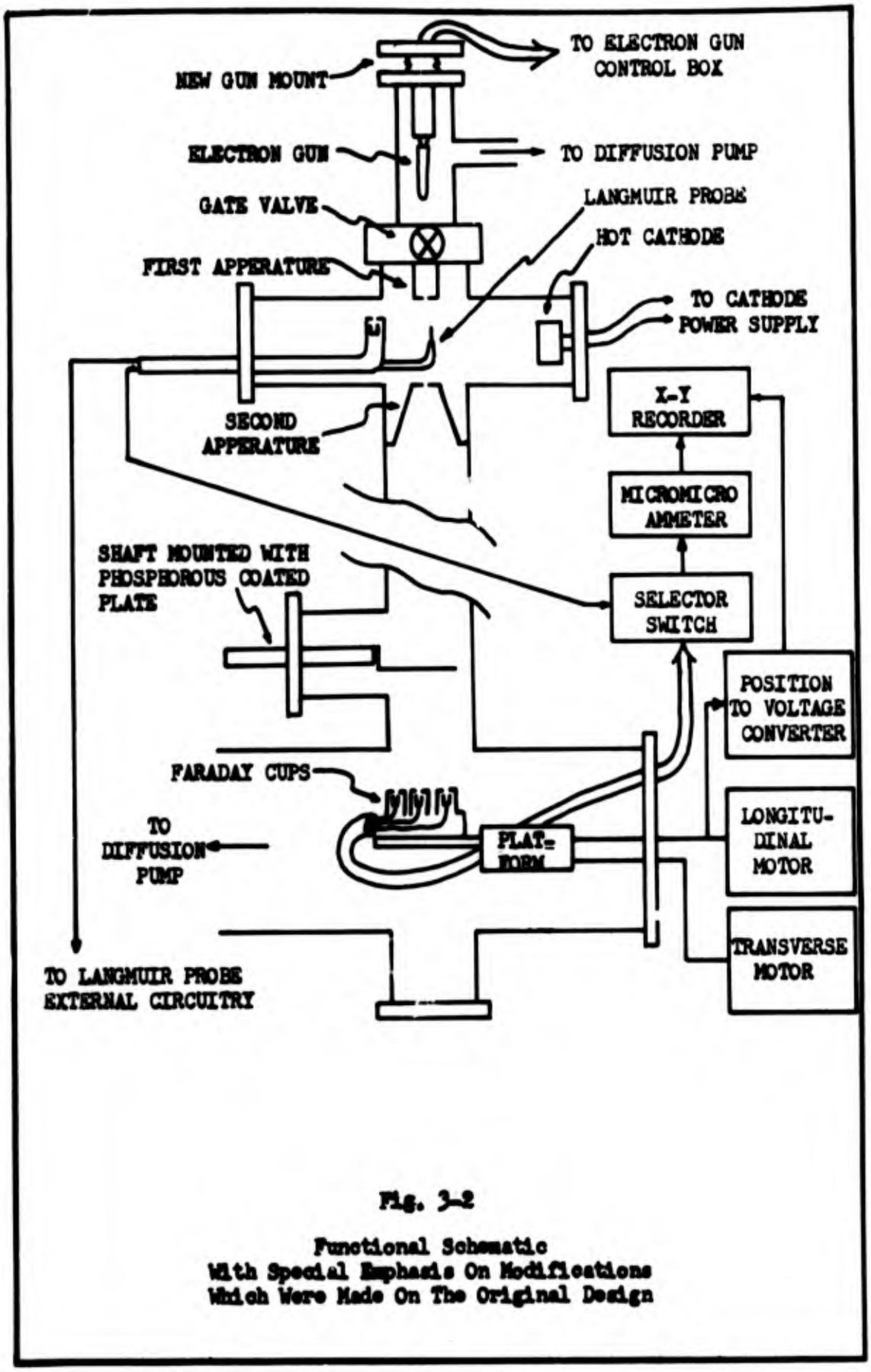

Fig. 3-2

Functional Schematic
With Special Emphasis On Modifications
Which Were Made On The Original Design

into the interaction chamber.

The interaction chamber contained the gas or plasma being studied, a Faraday cup to measure the electron beam as it entered the chamber, that is, the input current, a hot or cold cathode, and a Langmuir probe to measure plasma number densities and electron temperatures. It also contained a Pirani-gage probe to measure the pressure of the gas being studied and a needle valve to control the pressure of the flowing gas. After passing through the gas or plasma, the electron beam exited through a second apperature three millimeters in diameter.

The beam then passed through a 108 centimeter interaction-free zone at the end of which was attached the detection chamber. This chamber contained Faraday cups to measure the beam distribution and a moveable platform to which the cups were mounted. This chamber was kept at a pressure of 10^{-5} torr by a second diffusion pump. A micromicroammeter was used to measure the Faraday currents and a x-y recorder to graph the beam profile. The power supplies and additional measuring instruments are listed in Appendix D and require no description.

The description of the modifications made to this design are described here according to the chamber in which the change was made.

Gun Chamber

Prior to the present modifications, it was necessary to vent the entire apparatus to the atmosphere whenever any one section required that all pumps be turned off and the apparatus vented to atmospheric pressure. This was necessary even after the electron gun had been activated and repeatedly fired. Each time the gun was fired and then

the apparatus vented to atmospheric pressure, the gun's cathode became contaminated, which severely reduced its life.

Since it would be necessary on this project to vent the apparatus many times, a gate valve (Fig. 3-2 & 3-3) was placed between the interaction and gun chambers. This allowed the interaction and detection chambers, which contain the components worked on most frequently, to be opened while the gun chamber, and the electron gun, remained at the normal operating pressure of 10^{-8} torr. As a result, the normal gun life was increased from a few weeks to several months.

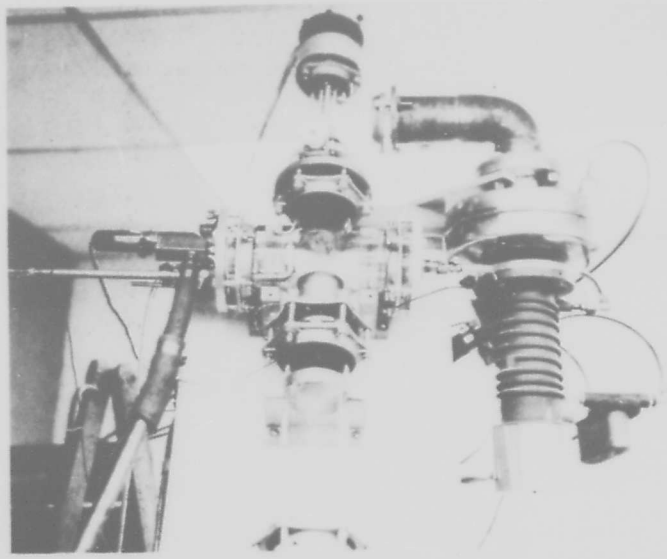

FIG. 3-3
GUN CHAMBER, GATE VALVE AND INTERACTION CHAMBER

To make the change, a new gun chamber was constructed using the same basic design. Since the gun chamber and gate valve had to fit into the space occupied previously by the original gun chamber design, it was necessary to make several other modifications. A shorter, smaller diameter T-shaped glass housing was used to meet the space

restriction. This in turn required the construction of a new electron gun mount (Fig. 3-4). This mount was similar to the original except an all metal construction was used. In addition, the first apperature was removed to save space and a new one built onto the bottom side of the gate valve assembly (Fig. 3-5). When finished, the entire assembly was mounted and aligned.

To eliminate several minor, but nuisance problems, the electron gun control apparatus was rebuilt. The basic design was not changed in any way, only the construction. The faulty wiring and spacing between the controls created some conditions hazzardous to the operator. These were eliminated by construction of a new control box. Several test jacks were added to provide easy measurement of potentials without exposure to the high voltages used. In addition, a quick disconnect system was put into the wires leading from the control box to the electron gun mount at the top of the apparatus. This allowed the electron gun mount to be separated from the control box during installation of a new gun.

Interaction Chamber

Very few changes were made in this chamber. The Faraday cup was moved closer to the first apperature to insure a more accurate measurement of the input beam current. Also, the Langmuir probe was moved to the center of the plasma to obtain a more relevant measurement of charged particle density.

After several cold cathode experiments were completed, a hot cathode was mounted in the interaction chamber. This cathode is commercially produced by General Electric for their GE 5544 thyratron

FIG. 3-4
GUN MOUNT AND GUN

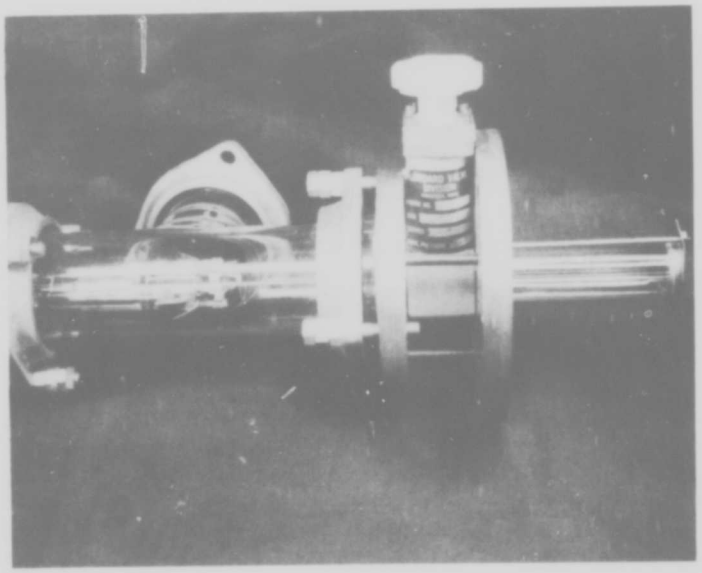

FIG. 3-5
GUN CHAMBER, GATE VALVE, AND FIRST APPERATURE

tube. Filament (heater) current was provided by a 0-20 ampere direct current power supply.

Detection Chamber

The original design of the detection system employed manual traversing of the Faraday cup, which was electrically connected to a micromicroammeter. The output of this meter was connected to an x-y recorder. Currents received by the Faraday cup were transformed into a voltage signal and plotted on the y-axis of the recorder. Position data, plotted on the x-axis, came from a potentiometer mounted on the Faraday cup slide shaft. The problem here was the inability to get a steady, slow rate of travel of the cup by hand. When traversing the beam, the unavoidably erratic motion caused rapid changes in the

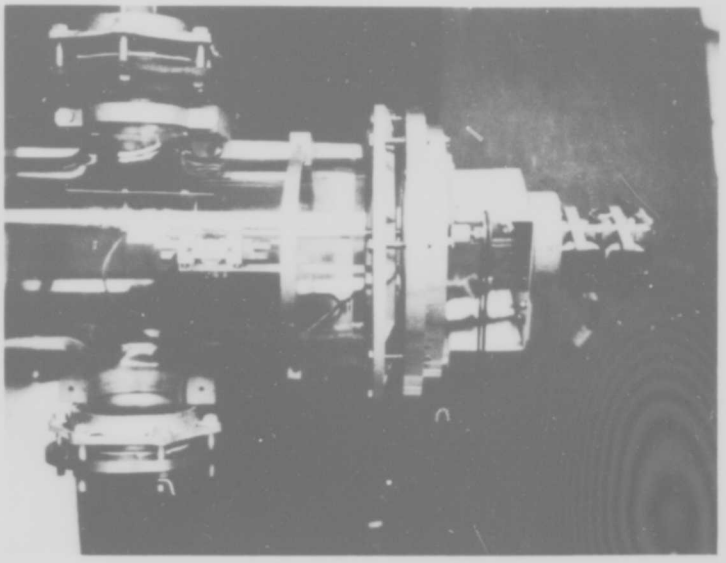

FIG. 3-6
DETECTION CHAMBER

currents received by the Faraday cup. Because of the micromicroammeter lag time constant, these rapid changes were not immediately indicated at the output. As a result, the profiles obtained were not reliable.

To overcome this, a motorized platform was designed and constructed. A new, larger diameter detection chamber was used (Fig. 3-6) and two drive motors obtained. The platform (Fig. 3-7 & 3-8) was constructed with two degrees of freedom. The motors were mounted externally and connected to the platform by means of flexible shafts. The longitudinal motor, controlling the platform travel along the chamber as seen facing the apparatus, moves the platform at a uniform rate of 0.4 inch per minute. This allows the micromicroammeter output to keep up with the input and eliminate the problem mentioned previously. The longitudinal motor was attached by pulley to a potentiometer which provided position information to the x-input of the x-y recorder.

The transverse motor moves the bed at a uniform rate of two inches per minute. This poses no problems since the Faraday cup measurements are made when the bed is moving in the longitudinal direction.

To perform the experiments, three Faraday cups were mounted on the platform. These cups were 0.26, 1.00 and 4.00 millimeters in diameter and were connected to an external selector switch. This in turn was connected to the micromicroammeter.

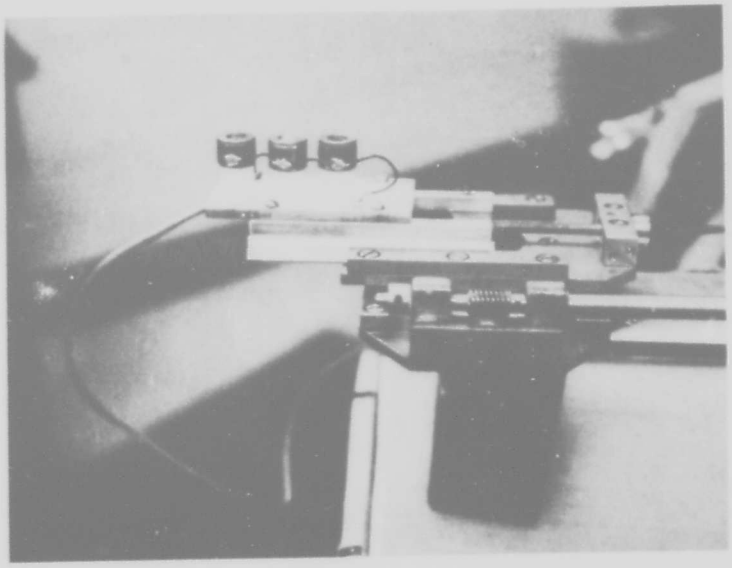

FIG. 3-7
TWO DEGREE OF FREEDOM PLATFORM AND FARADAY CUPS

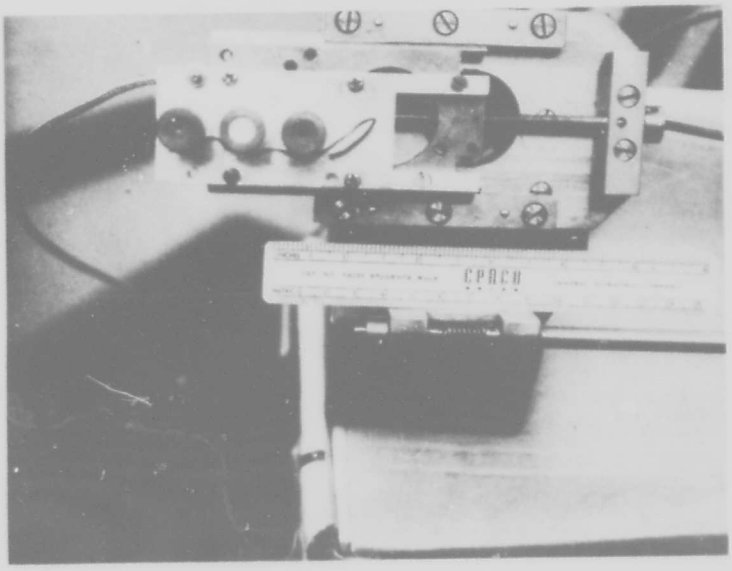

FIG. 3-8
DETECTION SYSTEM AS SEEN BY THE ELECTRON BEAM

IV. Single Scattering Experiment

Comments on the Experiment

In his work, Wawak conducted some initial scattering experiments using the small angle scattering device described in Chapter III. In one of these, the total scattering cross-section of argon gas was measured using a 1.6 Kev electron beam energy (Ref. 16:65). This result was then found to compare favorably with the Thomas-Fermi theory shown in Fig. 2-2. As a preliminary study, this experiment was continued with two intents. The first was to obtain total scattering cross-sections for other energies and detector sizes and look at the scaling. The second objective was to eliminate inefficient measurement techniques. This was done to reduce the time required to finish one measurement which initially required 40 to 50 minutes. The basic procedure followed is described in the next section, and, since the next experiment requires using this procedure twice for each measurement, it will be referred to in later sections.

Procedure

In all experiments described in this report, the initial chamber pressures were below the following values:

Gun Chamber	10^{-7} mm of Hg
Detection Chamber	10^{-5} mm of Hg

These pressures were repeatedly checked before and after the scattering gas was admitted into the interaction chamber, and if any change was observed the test was terminated and begun again. The basic measurement procedure used is as follows.

The electron gun filament power was turned on and the cathode

temperature allowed to stabilize. The beam produced was focused to pass through the one millimeter diameter first apperature shown in Fig. 3-2. After aligning the beam to pass through both the first and the three millimeter diameter second apperatures, a small aluminum plate was placed in its path in the detection chamber. This plate was lightly coated with phosphorous powder and provided a visual check of the beam. This was done to insure that no erratic behavior or undesired deflection of the beam was present.

After completing the beam alignment, argon gas was admitted into the interaction chamber and the pressure allowed to stabilize before any beam measurements were taken. The beam input current, before scattering, was measured at the first apperature, using a Faraday cup having a four millimeter apperature. Initially, an attempt was made to measure the beam profile after scattering at the detector section in every test. The proposed approach and reasons for abandoning it are discussed in Appendix A. Instead, fixed centerline detector current measurements were taken using 0.256, 1.0 and 4.0 millimeter diameter Faraday cups. The ratio of the detector current to the input current gave the non-dimensional detector current. All scatterer number densities were calculated using the perfect gas law and the interaction chamber pressure measured by a Pirani vacuum gage.

Results

For this experiment, only the beam energy and neutral gas pressure were varied. Beam energies of 1.5 Kev and 2.0 Kev were used while the pressure was varied from approximately 5 to 35 microns of mercury. Table II shows typical values obtained for a beam energy of 1.5 Kev

Table II

Typical Neutral Scattering Data

Pressure (microns of Hg)	XN ($\times 10^{15}$ per cm^{-2})	Detector Current ($\times 10^{-5}$ ma)	Input Current ($\times 10^{-5}$ ma)	$-Ln(I/I_o)$
9.8	3.34	1.040	2.00	0.65
13.0	4.43	0.068	0.14	0.72
13.5	4.60	1.380	2.73	0.68
16.0	5.45	1.000	2.40	0.88
16.0	5.45	0.400	1.70	0.85
17.0	5.79	0.900	2.73	1.08
20.0	6.81	0.850	2.74	1.17
21.0	7.17	0.100	0.23	0.83
21.0	7.15	0.800	2.73	1.23
23.0	7.83	0.730	2.72	1.32
23.0	7.83	0.730	2.72	1.32
24.0	9.17	0.064	0.22	1.23
25.0	8.51	0.600	2.73	1.52
26.0	8.85	0.440	2.75	1.83
28.0	9.53	0.480	2.43	1.74
29.0	9.87	0.038	0.25	1.88

NOTE: The above data is given for a beam energy of 1.5 Kev and a detector apperature diameter of 4.00 millimeter.

using the large (4.0 mm) cup.

This data was then interpreted by using the equation:

$$\ln(I_1/I_2) = S(N_2 - N_1)x \qquad (25)$$

where N_1 and N_2 are the number densities at two arbitrary neutral gas pressures

I_1 is the non-dimensional detector current at a density of N_1

I_2 is the non-dimensional detector current at a density of N_2

S is the total collision cross-section

x is the interaction distance which was held constant at eight centimeters.

Figures 4-1 and 4-2 show the semi-log plots of the data obtained during these experiments. From these plots, using Eq. (25), the following total cross-sections were obtained.

Table III

Measured Neutral Total Scattering Cross-Sections

Beam Energy (ev)	Measured Cross-sections (cm^2) 0.256 mm cup	1.0 mm cup	4.0 mm cup	Theoretical Cross-sections (From Fig. 2-2)
1500	4.3×10^{-16}	-	2.31×10^{-16}	5.2×10^{-16}
2000	3.3×10^{-16}	-	1.54×10^{-16}	4.5×10^{-16}

The small cup (0.256 mm diameter) total cross-sections compare very well with the Thomas-Fermi results. This can be fully appreciated when considering the fact that the Thomas-Fermi result overestimates cross-sections in the energy range considered. For a discussion of this overestimation, the reader is referred to Ref. 1:39. Both large

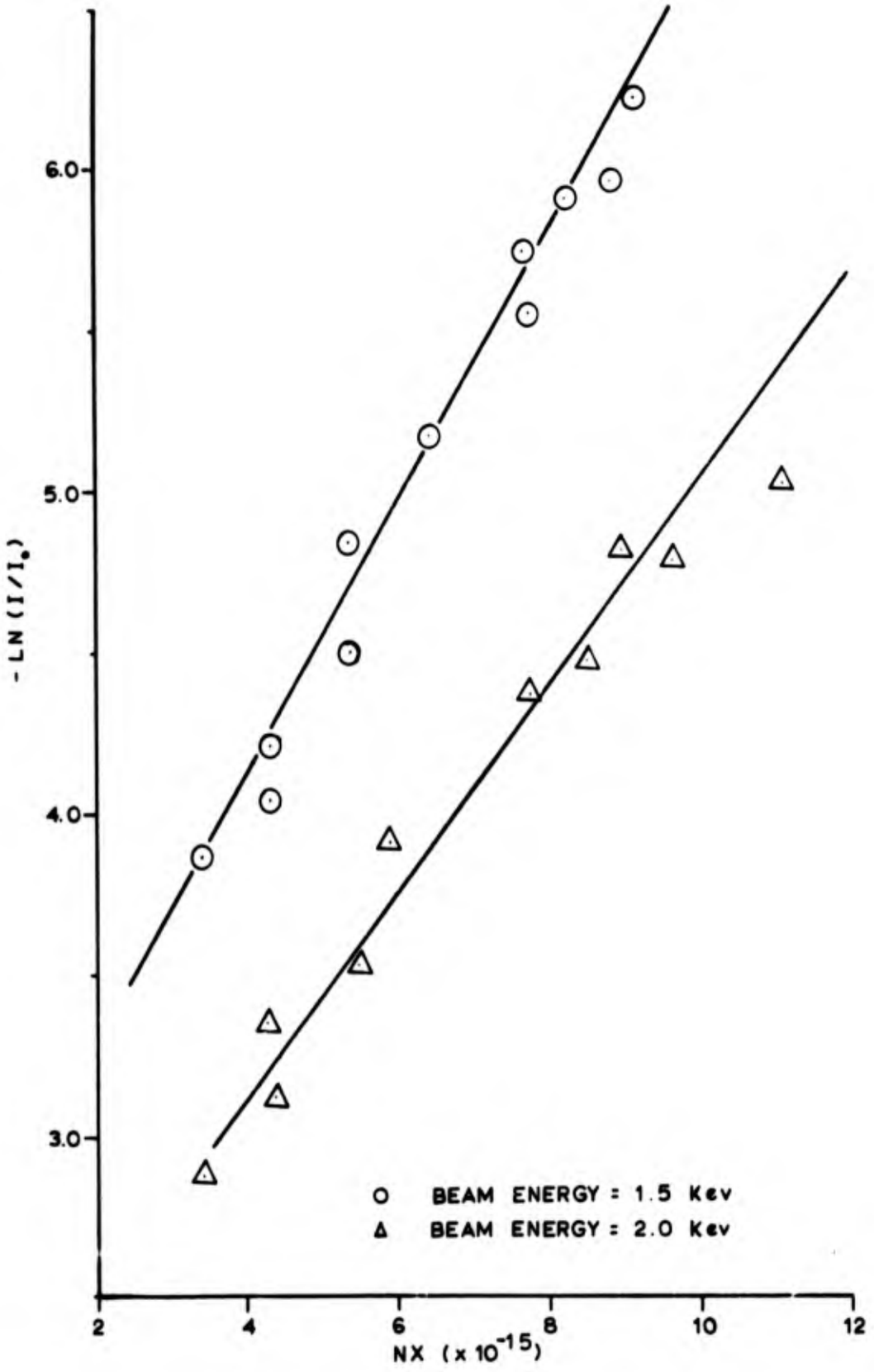

FIG. 4-1
DETERMINATION OF TOTAL CROSS-SECTIONS (SMALL CUP)

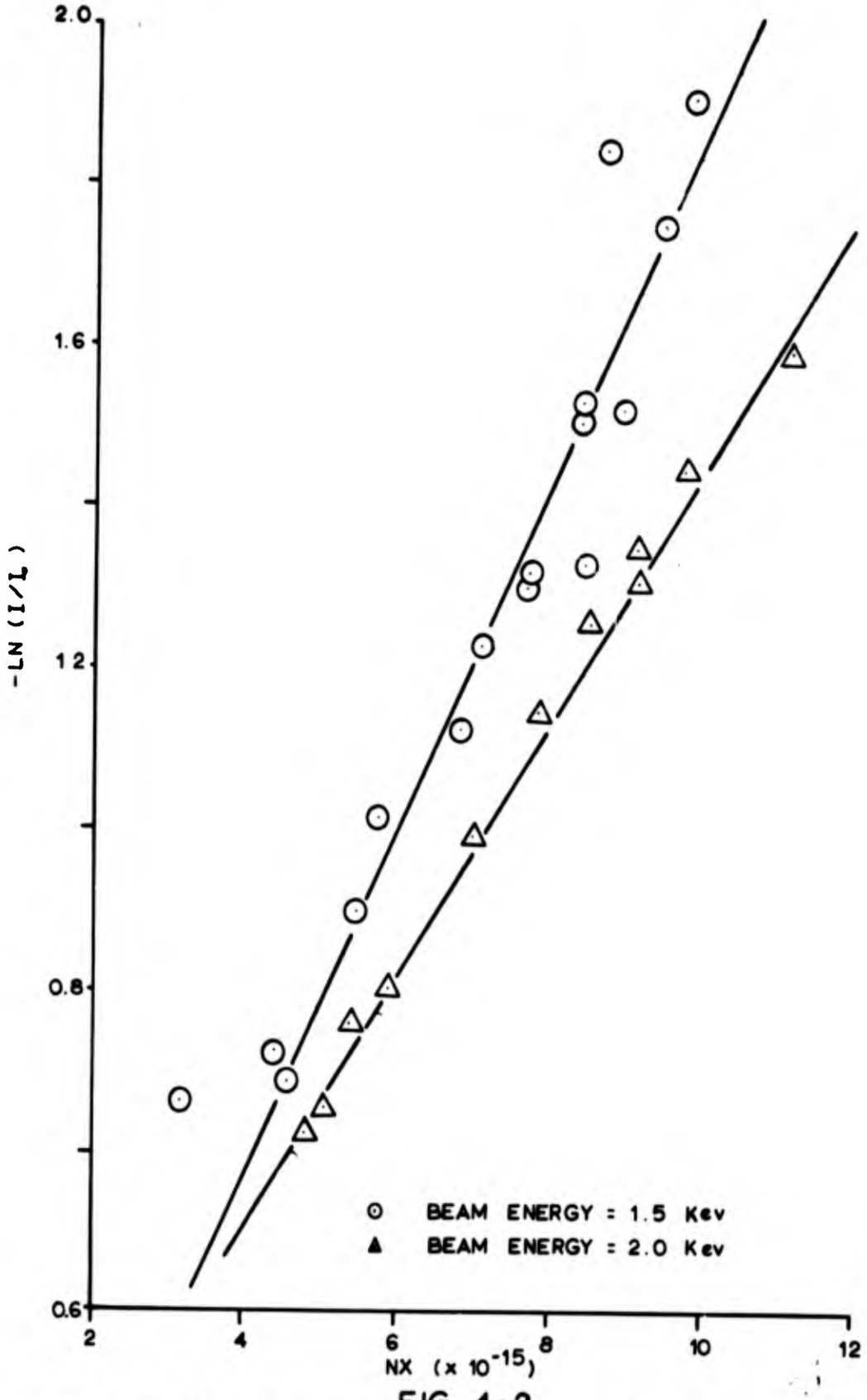

FIG. 4-2
DETERMINATION OF TOTAL CROSS-SECTIONS (LARGE CUP)

cup (4.0 mm diameter) values are approximately 28 per cent of the theoretical values. However, the small angle scattering device was not calibrated for non-ideal effects which are encountered in scattering experiments, therefore the values measured are considered to be in good agreement. A detailed discussion of these effects is available in Ref. 1:44 and will not be repeated here.

It is noted in Table III that no meaningful information was obtained from the medium cup (1.0 mm diameter) data. The very wide spread in the data points when plotted in the manner outlined did not permit any reasonable curve to be drawn. Since this occurred for both beam energies, it appears that the nearness of the cup diameter to the beam width causes accurate measurements to be very difficult to obtain (see Fig. A-1), or that some as yet undiscovered malfunctions occurred.

V. Multiple Scattering Experiment

Comments on the Experiment

The problem can best be understood by considering the scattering event. In neutral particle single scattering, only neutral atoms are present to scatter the electron beam. Thus, the problem is relatively simple. However, in plasma scattering both neutrals and charged particles are present. Thus, the charged particle scattering which occurs when the plasma is present cannot be inferred by the normalized detector current as was done in Chapter IV. As a summary of previous discussions of this problem (Ref. 1:8), one can say that the neutral particle scattering occurring in the plasma can be removed by

$$\left[\frac{I_d}{I_i}\right]_{\substack{\text{charged}\\ \text{particles}}} = \frac{\left[\frac{I_d}{I_i}\right]_{\text{plasma}}}{\left[\frac{I_d}{I_i}\right]_{\text{neutral}}} \tag{26}$$

where I_d is the detector current and I_i is the input current. Thus, if the neutral scattering normalized detector current is known, then the charged particle scattering can be found assuming no change in neutral scattering when the plasma is ignited.

In simple form, Eq. (26) is the multiple scattering experiment. The parameters involved were selected such that plural scattering dominated. The limitations placed on the definition of multiple scattering in Chapter II will be used here. That is, multiple scattering will imply the plural regime only. No statistical interpretation of multiple scattering will be discussed in this report.

The procedure used to obtain experimental multiple scattering data can be summarized in brief. The input and detector currents were measured for a neutral gas in the interaction chamber using the procedure described in Chapter IV. The ratio of the detector current to the input current gave the normalized plasma-off detector current, denoted in this section as I_o. In this experiment, the neutral pressure was maintained at 32.2 microns of mercury while the 0.256 millimeter cup was used to measure the detector current.

Next the plasma was ignited by a D.C. voltage applied across the cathode and anode located at each end of the interaction chamber. After the plasma had stabilized, the input and detector currents were measured following the procedure outlined in Chapter IV. The ratio of these currents gave the normalized plasma-on detector current, denoted here by I.

The ratio of the normalized plasma-on detector current to the normalized plasma-off detector current is defined as the survival current. The survival current is in reality the normalized detector current, considering only charged particle scattering.

After the plasma-on currents were measured, a Langmuir probe trace was taken to determine the plasma properties. This provided charged particle number densities determined by a method independent of the scattering experiment. A typical probe trace is shown in Fig. B-1. Using Laframboise's theory as outlined in Appendix II, the electron and ion number densities and the electron temperature were calculated from the observed probe trace.

The survival current defined above assumes no change in the neutral scattering between the plasma-off and the plasma-on operating

conditions. However, the plasma properties do not remain constant since production of the plasma either requires heating of the neutral gas and excites some of its atoms to metastable states, or produces this effect as an undesirable by-product (Ref. 1:11). Thus, it is necessary to calibrate the equipment to account for the change of neutral scattering due to these effects.

Neutral Background Heating Effect

From Fig. 2-2, it can be seen that for very large detector cups the charged particle scattering cannot be distinguished from neutral scattering. Thus, the scattering due only to neutrals in a plasma can be determined using a very large cup. To measure this experimentally, the procedure outlined in the previous section was used with the exception that no Langmuir probe trace was necessary. Instead of the 0.256 millimeter diameter detector cup, the 4.0 millimeter diameter detector cup was used to measure the detector current. It can be seen from Fig. A-1 that this cup is large as seen by the beam.

The normalized detector currents measured are defined as:

I_{hot} = normalized plasma-on detector current neglecting plasma scattering (i.e., using a large detector cup).

I_{cold} = normalized plasma-off detector current (i.e., neutral gas only, also using the same detector cup).

Thus,

$\frac{I_{hot}}{I_{cold}}$ = fraction change in current due to undesired heating of neutrals by the plasma.

Thus, the true survival current measured would be:

$$\frac{I}{I_o} = \left[\frac{I}{I_o}\right]_{recorded} \times \frac{I_{cold}}{I_{hot}} \qquad (27)$$

For this experiment, the value of I_{hot}/I_{cold} was measured as a function of plasma current. That is, the plasma current was used as the parameters for determining the correction factor to be used. These measurements were made using a cold and a hot cathode. For the cold cathode no correction factor was measurable for plasma currents up to 1.5 milliamperes. Unfortunately, plasma currents above 1.5 milliamperes were not possible due to the inability to maintain the plasma stable. However, correction factors for the hot cathode were measured for plasma currents up to 13.0 milliamperes. A graph of these results is shown in Fig. 5-1 for a filament current of 14.2 amperes. Some unusually high and low values were measured but were discarded as being due to measurement errors.

It can be seen in Fig. 5-1 that a near constant correction value exists from zero to four milliamperes plasma current. Because the normalized plasma-off current was measured with the heater off, this indicates the heating due to the heater alone. The accuracy of this can be shown by obtaining calibration curves for various heater currents. A second calibration curve was obtained for a heater current of 16.0 amperes and is shown by the dashed line in Fig. 5-1.

Cold Cathode Results

In the beginning, cold cathode D.C. plasma discharges were used to obtain multiple scattering data. The cathode was oriented so that the electron beam passed through the positive column of the plasma. This was necessary because of the extreme difficulty encountered in finding the zero electric field regions of the plasma. As shown in

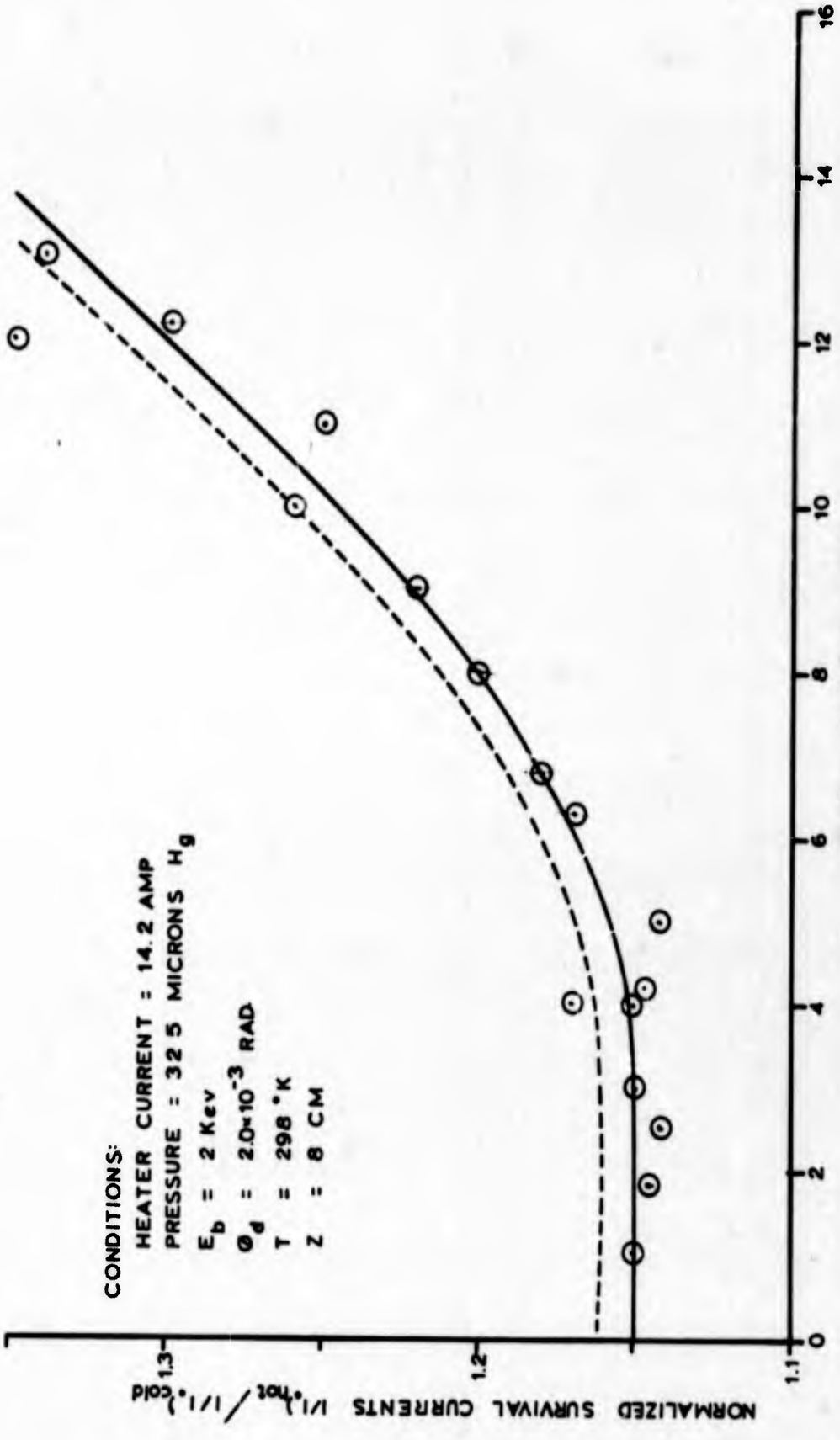

FIG. 5-1
CALIBRATION FOR NEUTRAL GAS HEATING (HOT CATHODE)

Fig. 5-2, a high field exists on either side of these regions and it caused severe deflection of the electron beam when the cathode was not positioned exactly. Although a field did exist in the positive column, it was not very strong and caused no problems.

The procedure used in obtaining cold cathode data was discussed earlier, however the 0.256 millimeter diameter detector cup was used to measure detector currents. From the plasma-on and plasma-off normalized detector current measurements and the Langmuir probe trace, the survival current and number densities were obtained. Typical data measurements and calculated results are shown in Table IV. Note that the electron number densities are very much less than the ion number densities. In calculating these number densities, correction factors were determined according to procedures outlined by Sonin (Ref. 14). The nature of the probe trace and the corrections calculated indicated that the ion number densities were more accurate. Thus the total number density, ion plus electron, was taken as twice the calculated ion value.

The calculated results for the cold cathode data are plotted in Fig. 5-3. The non-dimensional survival current is plotted versus scatterer number density in particles per cubic centimeter. Some spread in the results is noted and this can be attributed, in part, to systematic errors. Also noted is the lack of data in the high number density range, i.e., above 10^{10} per cubic centimeter. This was caused by the inability to get a sufficiently dense plasma without arcing. This resulted in the data being clustered at the top of the theoretical curve. It was desired to get survival currents in the 0.1 to 0.8 range in order to make a meaningful comparison to the Moliere theory.

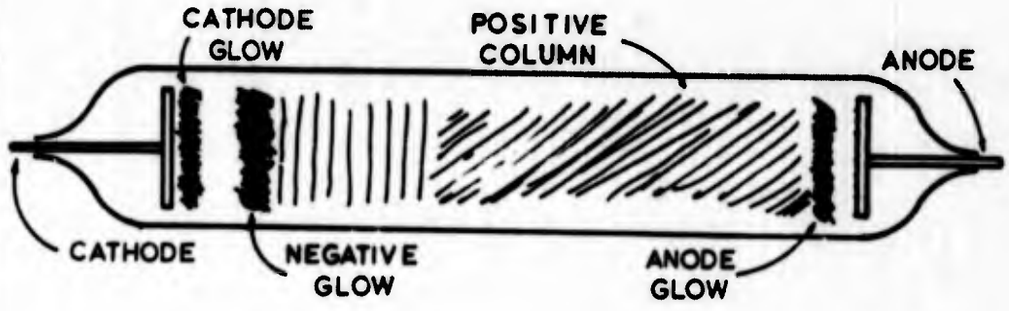

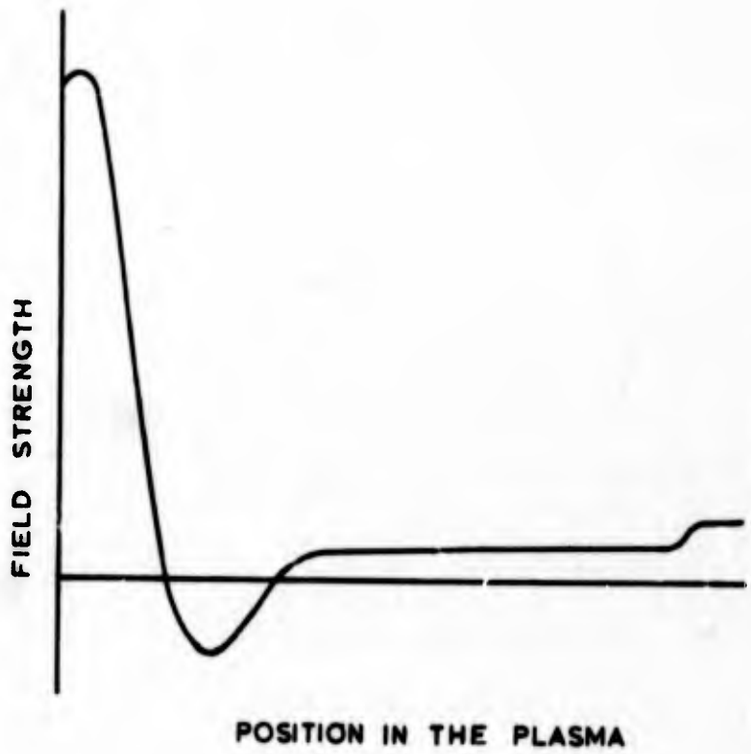

FIG. 5-2
QUALITATIVE DESCRIPTION
OF THE PLASMA FIELD STRENGH

Table IV

Typical Cold Cathode Charge Particle Scattering Data

$\frac{I/I_o)_{on}}{I/I_o)_{off}}$	Ion Number ($\times 10^9$ cm^{-3})	Electron Number ($\times 10^9$ cm^{-3})	Electron Temperature (^oK)
0.961	3.02	0.64	4540
0.478	7.22	2.49	5550
0.840	4.11	1.59	5550
0.740	3.41	0.52	4540
0.854	5.07	1.76	6057
0.932	1.65	0.32	5550
0.851	3.80	0.90	6050
0.950	1.65	0.21	5550
0.800	2.18	0.36	6560
0.880	2.71	0.41	6060
0.750	2.59	0.50	6060
0.970	2.83	0.49	6060

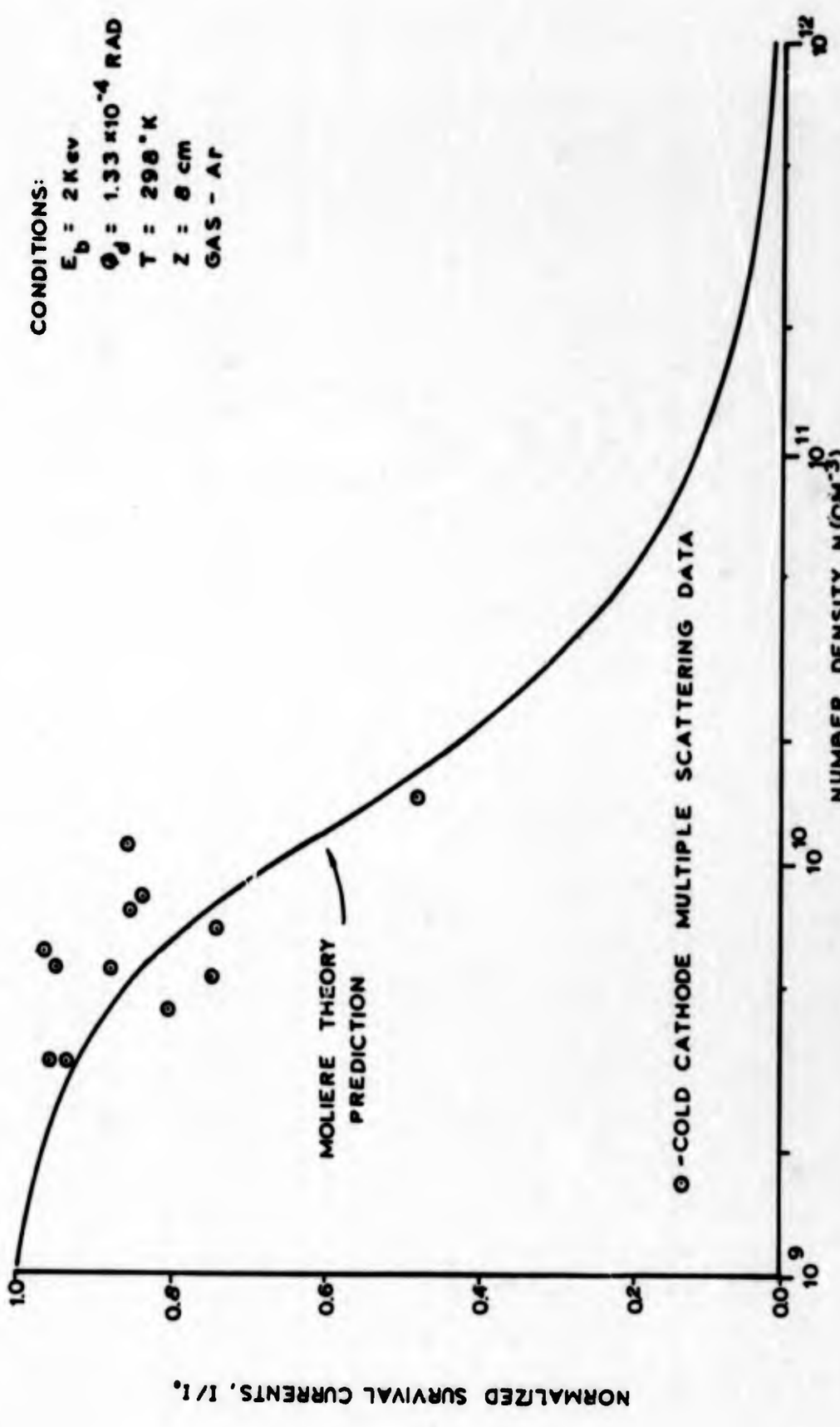

FIG. 5-3
THEORETICAL AND EXPERIMENTAL
MULTIPLE SCATTERING VALUES (COLD CATHODE)

This could have been done by reducing the detector cup size, resulting in lower measured survival currents. In this case, the theoretical curve, discussed in Chapter II, would have moved to the left and a comparison to theory could have been obtained for the survival current range desired. To do so would have required reducing the detector cup size from 1.33×10^{-4} radians to approximately 2.0×10^{-5} radians. This would necessitate a detector cup with a diameter of about 0.038 millimeters. While this could have been done, it was decided instead to use a hot cathode to overcome the problem.

Hot Cathode Results

To overcome the low density problem mentioned in the last section, a General Electric 5544 thyratron cathode was installed in the interaction chamber. Filament current was provided by an improvised zero to twenty ampere power supply. The cathode was activated at a filament heater current of 12 amperes for a period of 24 hours. At regular intervals, the filament current was increased to 20 amperes for brief periods.

Once operating effectively, the cathode filament was turned off. The electron beam was focused and aligned and the normalized plasma-off current determined in the manner described earlier. When completed, the filament current was turned on and set at 14.2 amperes with the neutral gas pressure still set at 32.5 microns of mercury. While the gas warmed, the neutral pressure, measured by a Pirani vacuum gage, was watched closely. No noticeable change in pressure occurred. The filament temperature was checked using an optical pyrometer and found to be about 1700 degrees centigrade.

After sufficient time had been allowed for heating the gas, the plasma voltage was applied. The input and detector currents were measured and recorded, and a Langmuir probe trace was taken. The survival current was then calculated using the data recorded. To account for the heating of the neutral background gas, the correction factor found previously was applied. The correction used was found in Fig. 5-1 according to the plasma current measured during each test. The corrected survival currents thus calculated were plotted and are shown in Fig. 5-4. All values were found to be 10 to 50 per cent above the values predicted by the Moliere theory. Noticeable on the graph is the lack of experimental data in the 10^{11} to 10^{12} particles per cubic centimeter number density range. As was the case in the cold cathode measurements, the inability to maintain a stable plasma for any length of time at these densities restricted the operating range. The cause for this action is not definitely known.

In addition, several interesting observations were made during this phase of the experiment and should be noted here. The ion and electron number densities were found to be very near equal as would be expected. This was not the case in the cold cathode experiment. As a result, the total number density used here consists of ion plus electron.

Also, at higher filament current, it was found that the plasma current did not change appreciably as the plasma voltage was varied from 200 volts to 4000 volts. However, very slight changes in filament current did cause very significant changes in plasma current. This filament current dominance of the plasma was particularly noticeable at filament currents above 16 amperes.

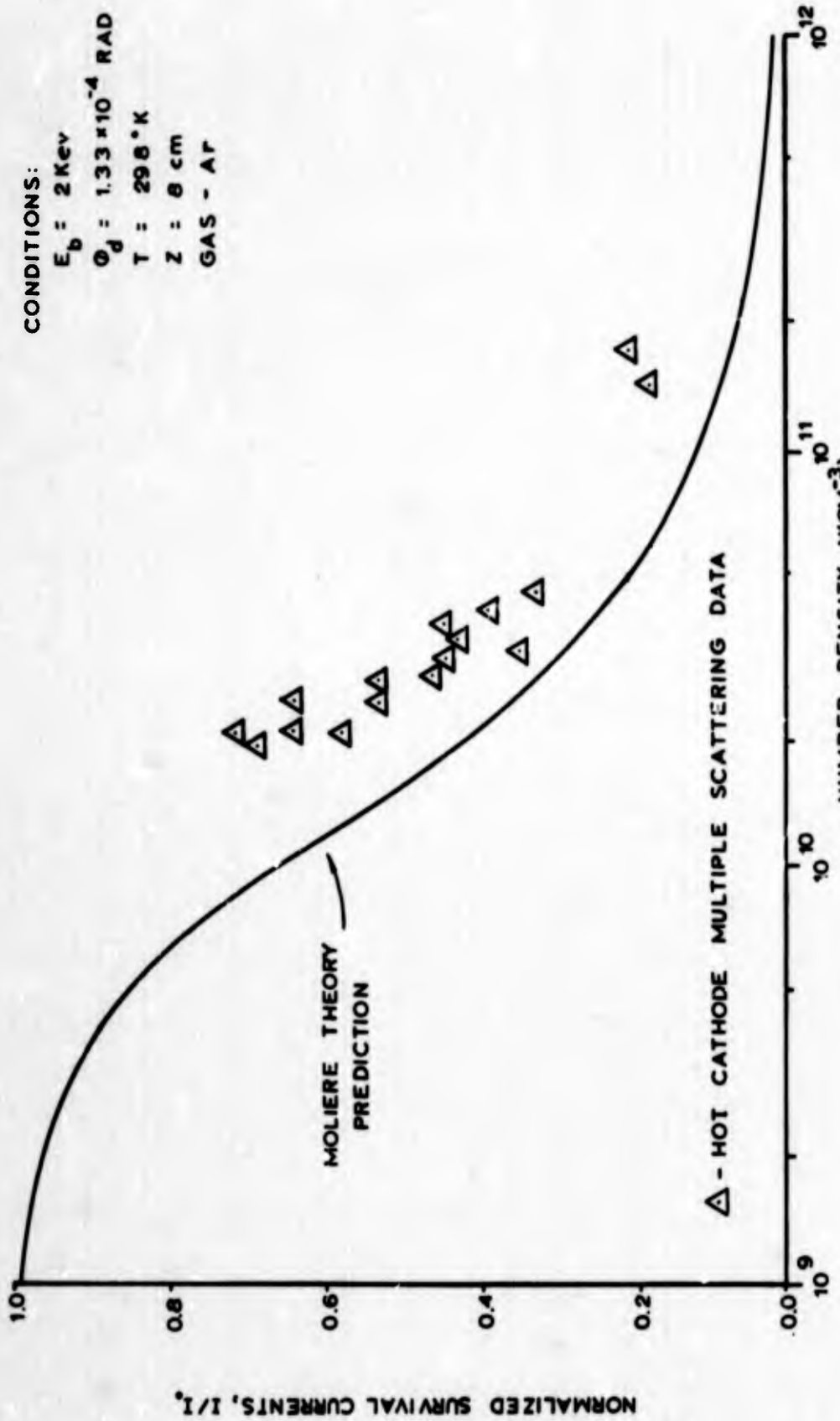

FIG. 5-4
THEORETICAL AND EXPERIMENTAL
MULTIPLE SCATTERING VALUES (HOT CATHODE)

It was also observed that the interaction chamber walls became deposited almost immediately with a dark film. With prolonged use, this deposit became even greater until a large section of the chamber was completely coated. Upon completion of the experiment, the chamber was opened and some of the deposits removed. Although no equipment was available for analyzing the deposit, it is suspected to be oxide deposits from the filament and some diffusion pump oil derivatives.

During the later stages, the arcing of the plasma which prevented the generation of higher number densities began occurring more frequently. This continued until eventually a heater setting of 14.2 amperes could not be obtained with arcing. Since a new calibration curve would be necessary if a new filament current setting were used, it was decided to terminate the experiment here.

Summary

As noted previously the experimental data shows some spread in the cold cathode results. However, when this data is combined with the hot cathode results, a very reasonable trend can be indicated. This trend is shown in Fig. 5-5 by the center line and resembles that shown for the Moliere theory. The dashed lines indicate the range of values the data could have taken due to uncertainties in the measurements.

It was noticed in all the data that the observed electron temperatures were less than half the values predicted by theory, which are approximately 17,000 degrees Kelvin (Ref. 5). Hot cathode measurements, shown in Table V, yielded temperatures in the range 5500 to 7500 degrees Kelvin while 5500 to 6500 degrees Kelvin were measured for the cold

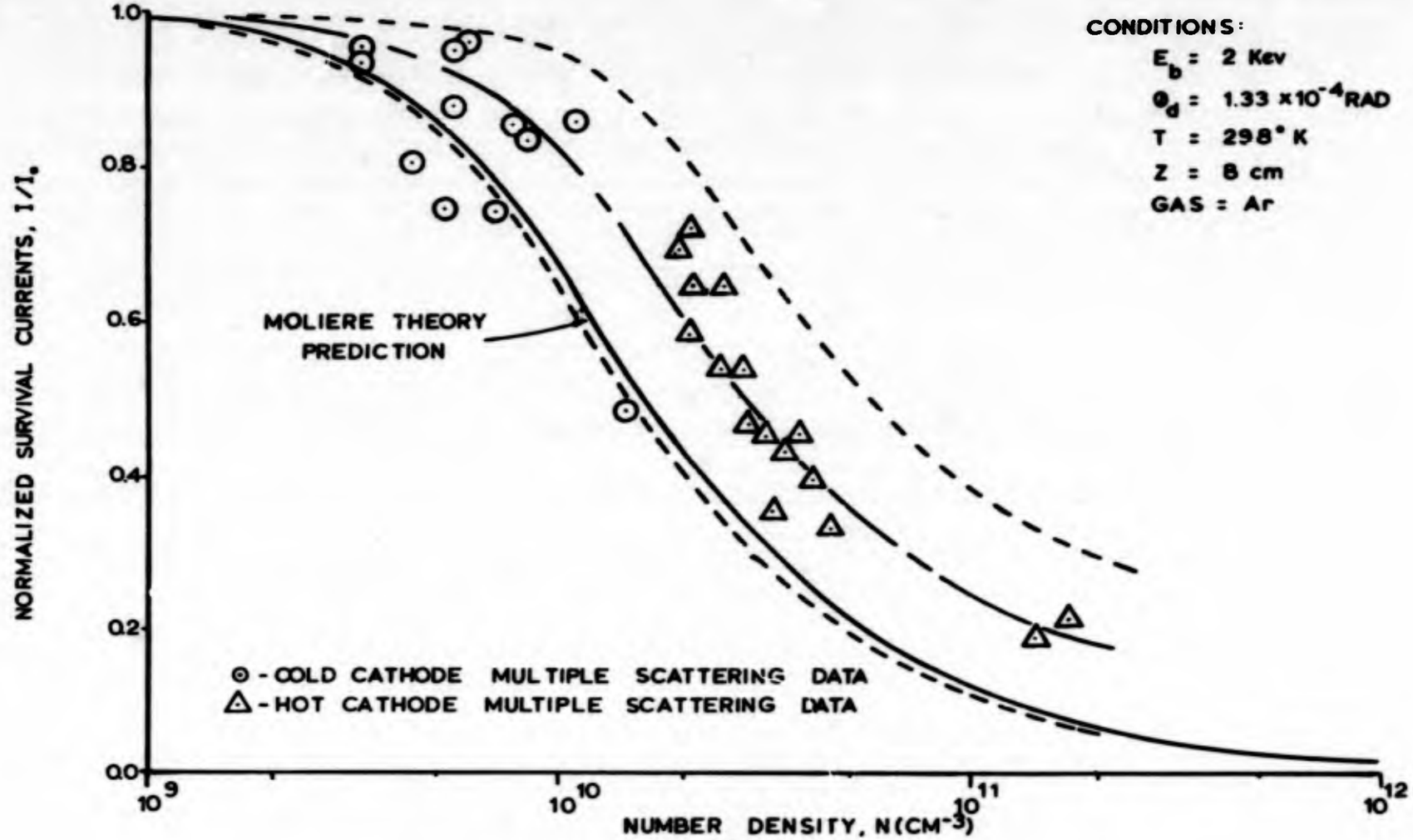

FIG. 5-5
THEORETICAL AND EXPERIMENTAL
MULTIPLE SCATTERING VALUES (COMBINATION)

Table V

Typical Hot Cathode Charge Particle Scattering Data

$\frac{I/I_o)_{on}}{I/I_o)_{off}}$ Uncorrected	$\frac{I/I_o)_{on}}{I/I_o)_{off}}$ Corrected	Ion Number ($\times 10^9$ cm^{-3})	Electron Number ($\times 10^9$ cm^{-3})	Electron Temperature (^oK)
0.413	0.347	1.46	1.75	6060
0.624	0.538	1.05	1.42	7070
0.622	0.533	1.10	1.68	7570
0.538	0.444	1.51	2.25	6560
0.507	0.423	1.42	2.00	6560
0.288	0.216	14.28	2.75	7570
0.521	0.442	1.18	1.89	6560
0.538	0.461	1.28	1.56	6060
0.237	0.185	11.28	2.75	7570
0.794	0.690	0.96	0.96	6060
0.657	0.570	0.83	1.22	6060
0.400	0.322	2.17	2.23	7070
0.735	0.640	0.84	1.26	5550
0.750	0.651	1.12	1.38	6060
0.473	0.388	1.61	2.32	5050
0.812	0.716	0.97	1.04	5050

cathode. A contamination study being conducted in the same department indicates that air and some other contaminants severely reduce the measured electron temperature of the plasma (Ref. 15). The results of this study show that the measured electron temperature drops to approximately 50 per cent of the theoretical value for very small percentages of contaminants. Measurements of relatively pure argon produce very good agreement with theory, thus the low electron temperatures observed in this study were not unexpected.

VI. Conclusions and Recommendations

The neutral single scattering experiment offers additional evidence as to the applicability of beam scattering techniques for determining neutral gas number density. Since secondary effects were not considered, the data is not expected to be highly accurate. However, the data obtained are in reasonable agreement with theory, thereby validating the general procedures and instrumentations. Moreover, the neutral measurements required later were used with much greater assurance of obtaining reasonable results from the apparatus.

The multiple scattering experiment indicates that charged particle number densities can be inferred from beam scattering techniques using the Moliere theory. However, in order to make the method available for general usage one should obtain data for other beam energies, detector sizes, interaction distances, and pressure settings. If the results, when plotted as shown in Fig. 5-5, agree as well as these, then it can be concluded that this is definitely a valid technique for general usage.

Should the same type of apparatus be used, the following recommendations may be of interest.

a) From the beam behavior, it appeared that space charge effects were present. The use of shielding of some sort around the walls of the apparatus may eliminate this(1). Also, the displacement of the detector platform introduced slightly irregular beam movement. This appeared to be caused by the fields set up by the Faraday cup apperatures (screen grids) being at 45 volts negative while everything

(1) Suggested by G. K. Medicus (Private Communication).

else was grounded (see Figs. 2-7 and 3-8). Using a relatively large flat plate drilled to form the three apperatures could possibly eliminate these beam deflections by presenting a uniform potential to the on-coming beam(2).

b) The gun mount used here allowed some unwanted electron gun deflections. This was due to a lack of gun mount rigidity. In the present system the electron gun is supported by the electrical leads only (see Fig. 3-4). The previous design held the gun securely by its glass stem. The latter is more desirable and should be used.

c) The hot cathode offered the best means for getting the desired scattering survival current range. However, plasma current instability was a problem. Use of a current regulator device in the plasma voltage circuit was tried in the latter stages of this project but it was a prototype system and did not produce the desired results. A properly designed current regulator could offer significant advantages.

d) Any future experiments should calibrate the equipment for non-ideal effects such as finite beam size, leakage of plasma through the apperatures, and space charge effects. For accuracy of results, any future experiment should undertake these necessary calibrations.

e) The detector platform's rate of longitudinal travel was too slow. The present motor was obtained through trial and error testing of discarded equipment. The desired detector speed would permit a complete traverse of the beam profile in approximately 20 seconds. Proper gearing of the present system could achieve this, however, a slightly higher speed, high torque direct drive system would be simpler.

---

(2) Suggested by John Moonan (Private Communication)

Bibliography

1. Battle, E. L. "Experiment on the Application of Electron Scattering to Plasma Diagnostics." University of Toronto Institute of Aerospace Studies Report No. 120. Toronto: University of Toronto, December, 1966.

2. Bethe, H. A. "Moliere's Theory of Multiple Scattering." Physical Review, 89:1256-1266 (1953).

3. Bowker, A. H. and G. J. Lieberman. Engineering Statistics. New Jersey: Prentice-Hall Inc., 1959.

4. Case, C. T. and E. L. Battle. "Moliere's Theory of Multiple Collisions Applied to the Scattering of an Electron Beam Injected Into a Plasma." Air Force Institute of Technology Technical Report 67-16. Wright-Patterson Air Force Base, Ohio: Air Force Institite of Technology, September 1967.

5. Cobine, J. D. Gaseous Conductors, Theory and Engineering Application. New York: Dover Publications, 1958.

6. Goudsmit, S. A. and J. L. Saunderson. Physical Review, 57, 24 and 58:24 (1950).

7. Kennard, Earle H. Kinetic Theory of Gases (Fourth Edition). New York: McGraw-Hill, Inc., 1938.

8. Laframboise, J. G. "Theory of Spherical and Cylindrical Langmuir Probes in a Collisionless, Maxwellian Plasma at Rest." University of Toronto Institute of Aerospace Studies Report No. 100. Toronto: University of Toronto, 1966.

9. Lewis, H. W. Physical Review, 78:526 (1950).

10. McDaniel, Earl W. Collision Phenomena in Ionized Gases. New York: John Wiley and Sons, Inc. 1964.

11. Moliere, G. Z. F. Naturforsch, 3a:78 (1948).

12. Mott, N. F. and H. S. W. Massey. The Theory of Atomic Collisions (Third Edition). Oxford: Clarendon Press, 1949.

13. Snyder, H. and W. T. Scott. Physical Review, 76:220 (1949).

14. Sonin, A. A. "The Behavior of Free Molecular Cylindrical Langmuir Probes in Supersonic Flows and their Application to the Study of the Blunt Body Stagnation Layer." University of Toronto Institute of Aerospace Studies Report No. 108. Toronto: University of Toronto, 1965.

15. Thomas, Timothy T. "An Experimental Study of the Effects of

Surface and Gas Contamination on Langmuir Probe Measurements." Air Force Institute of Technology Thesis No. GA/Phys/69-6. Wright-Patterson Air Force Base, Ohio: Air Force Institite of Technology, 1969.

16. Wawak, Stephen, Jr. "Design and Development of a Beam/Plasma Interaction Apparatus." Air Force Institite of Technology Thesis No. GA/Phys/68-4. Wright-Patterson Air Force Base, Ohio: Air Force Institite of Technology, 1968.

Appendix A

Proposed Numerical Integration Technique

The determination of scattering cross-sections for both single and multiple collision theories was accomplished using three Faraday cups in the detector section and an input cup in the interaction chamber. For given set of experimental conditions it is possible to obtain more data from each test by using a finite integration technique.

By using the small (0.26 millimeter diameter) detector cup, a fairly accurate profile of the beam can be obtained. This profile is assumed to be the profile observed on any plane passing through the beam axis. Shown in Fig. A-1 is a typical profile of the electron beam after it has passed through a neutral gas.

To determine the survival current for any detector size, use

$$I = \int_0^{A_d} \phi_{(r)} dA \qquad \text{(A-1)}$$

where A_d is the detector apperature area and $\phi(r)$ is the flux distribution as a function of radius. To perform this integration, use a finite integration technique and the profile obtained using the small cup. This profile is given in terms of the current received by the small cup at a position r. To obtain the flux

$$\phi = I_p/A_d = I_p/\pi r_d^2 \qquad \text{(A-2)}$$

where I_p is the profile current reading at a point (r) for the small cup.

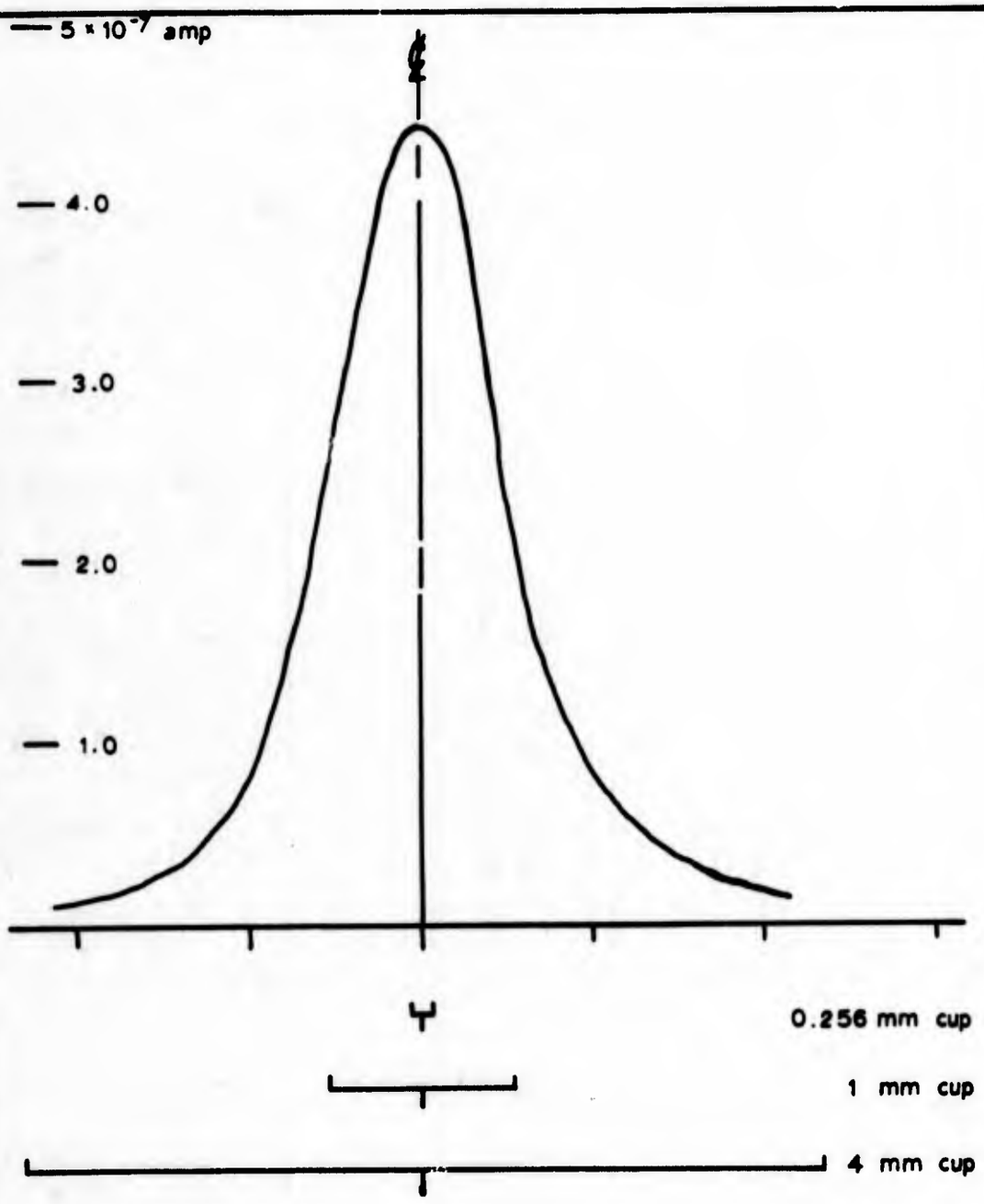

11 DEC '68

PRESSURE	16.0 MICRONS	MED. CUP	5.0×10^{-6} amp
X SCALE	0.5 VOLT/IN	LARGE CUP	$1.7\ 10^{-6}$ amp
BEAM ENERY	1500 eV	INPUT CUP	2.4×10^{-5} amp
Y SCALE	0.5 VOLT/IN	C/L PEAK	4.2×10^{-7} amp

FIG. A-1
TYPICAL BEAM TRACE IN NEUTRAL GAS

Thus the finite integration is accomplished by

$$I = \int_0^{r_d} (I_p/c) 2\pi r dr \qquad (A-3)$$

where C is the constant πr_d^2, or

$$I = [I_p(r + \delta r) - I_p(r)][2r + \delta r \;\; \delta r]_0^{r_d} \qquad (A-4)$$

where δr is the small increment of r. When the above calculated current is divided by the input current I_o the current ratio is obtained. This simple integration procedure will provide a great number of data points when applied to different detector sizes.

To check the accuracy of this technique, several integrations were performed using the medium and large Faraday cup radii as r_ds. These values were then compared with the measured detector currents. Since the small cup does provide a fairly accurate beam profile, it was expected that the integrated values would agree with the measured values. In all cases but two the measurements were within 10 per cent of the integrated values. The two exceptions can be attributed to possible misalignment of the small Faraday cup when the profile was taken.

These results were obtained early in this project and show the feasibility of the technique. However, in order to obtain one profile several measurements were necessary. This was because the electron beam displayed erratic behavior when the platform was traversed across the beam. This resulted in inaccurate profiles or in discontinuities appearing in the profile. Also, the excessive time required for one profile measurement allowed the beam conditions time to change slightly,

again rendering the measurement useless. Since no solution was apparent at that time without again modifying the system, this technique was abandoned.

Appendix B

Summary of Langmuir Probe Data Reduction Technique

Laframboise's theory of collisionless probes (Ref. 8), as treated by Sonin (Ref. 14), provides the calculation procedure for determining the electron temperature and charged particle number density from a Langmuir probe trace. The numerical data, in MKS units, are appropriate for cylindrical probes and atomic argon ions.

For a complete treatment of Laframboise's theory, the reader is referred to Sonin. In this report only the calculation procedure outlined by Sonin need be discussed. For simplification, the following definitions are made:

j_i and j_e	are the absolute magnitudes of the ion and electron current densities at the probe surface respectively.
N	is the charged particle number density in the undisturbed plasma.
T_e	is the electron temperatures.
γ_d	is the Debye length.
R_p	is the probe radius.
L	is the probe length.
K	is the Boltzmann constant.
e	is the magnitude of the electronic charge.
V	is one probe potential.
I_i	is a dimensionless ion current calculated by Laframboise.

Shown in Fig. B-1 is a typical Langmuir probe trace taken for a weakly ionized plasma. The x-axis records the probe potential and the y-axis the probe current. The electron probe current, j_e, is shown in

FIG. B-1
TYPICAL LANGMUIR PROBE CURVES
OF A WEAKLY IONIZED ARGON PLASMA

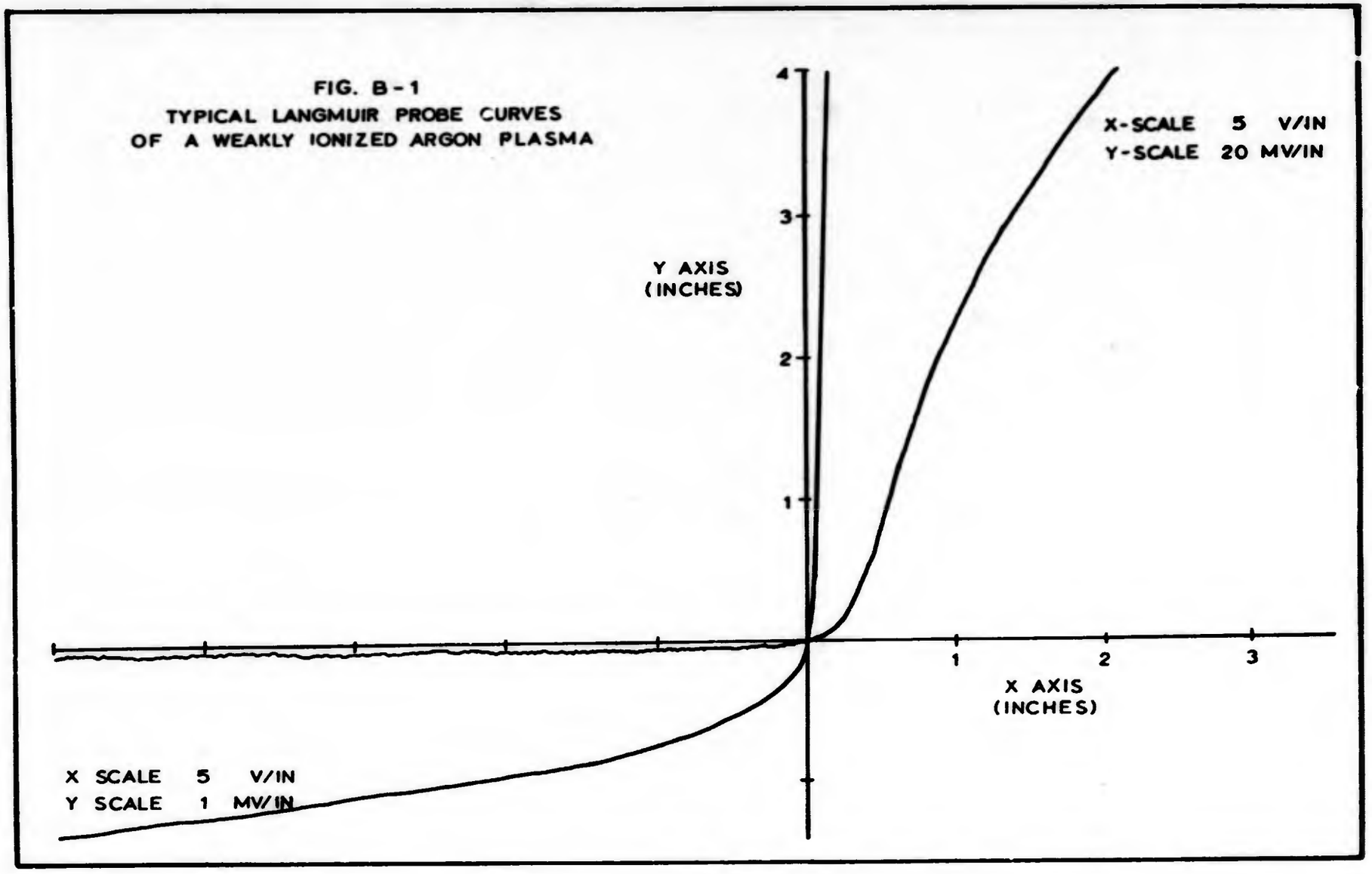

the first quadrant while the ion probe current, j_i, is in the third. The point where the trace crosses the axis, arranged at the coordinate center, is defined as the floating potential point, X_f. All potential measurements are made with respect to this point. The following procedure is used to determine the electron temperature and the charged particle number densities from this trace.

(1) Make a plot of Ln j_e versus V

(2) Determine KT_e/e from

$$\frac{d(\ln j_e)}{dV} = \frac{1}{(KT_e/e)} \tag{B-1}$$

(3) Determine the electron temperature in degrees Kelvin from

$$T_e = (1.1609 \times 10^{-3})(KT_e/e) \tag{B-2}$$

(4) Measure the ion probe current, J_i, at $10(KT_e/e)$ volts below X_f and calculate the current density in amperes/m^2 using

$$J_i(X_f - 10) = J/2\pi R_p L \tag{B-3}$$

(5) Calculate the quantity

$$\frac{R_P}{\lambda_d} I_i(X_f - 10) = 1.83 \times 10^8 \, R_p^2 \, \frac{J_i(X_f - 10)}{(KT_e/e)^{3/2}}$$

$$\frac{1.45 \times 10^7}{L/D} \quad \frac{J(X_f - 10)}{(KT_e/e)^{3/2}} \tag{B-4}$$

where D is the probe diameter.

(6) Determine the value of $I_i(X_f - 10)$ from Fig. B-2. Note: For all probe calculations in this study, the value of $I_i(X_f - 10)$ was 4.3.

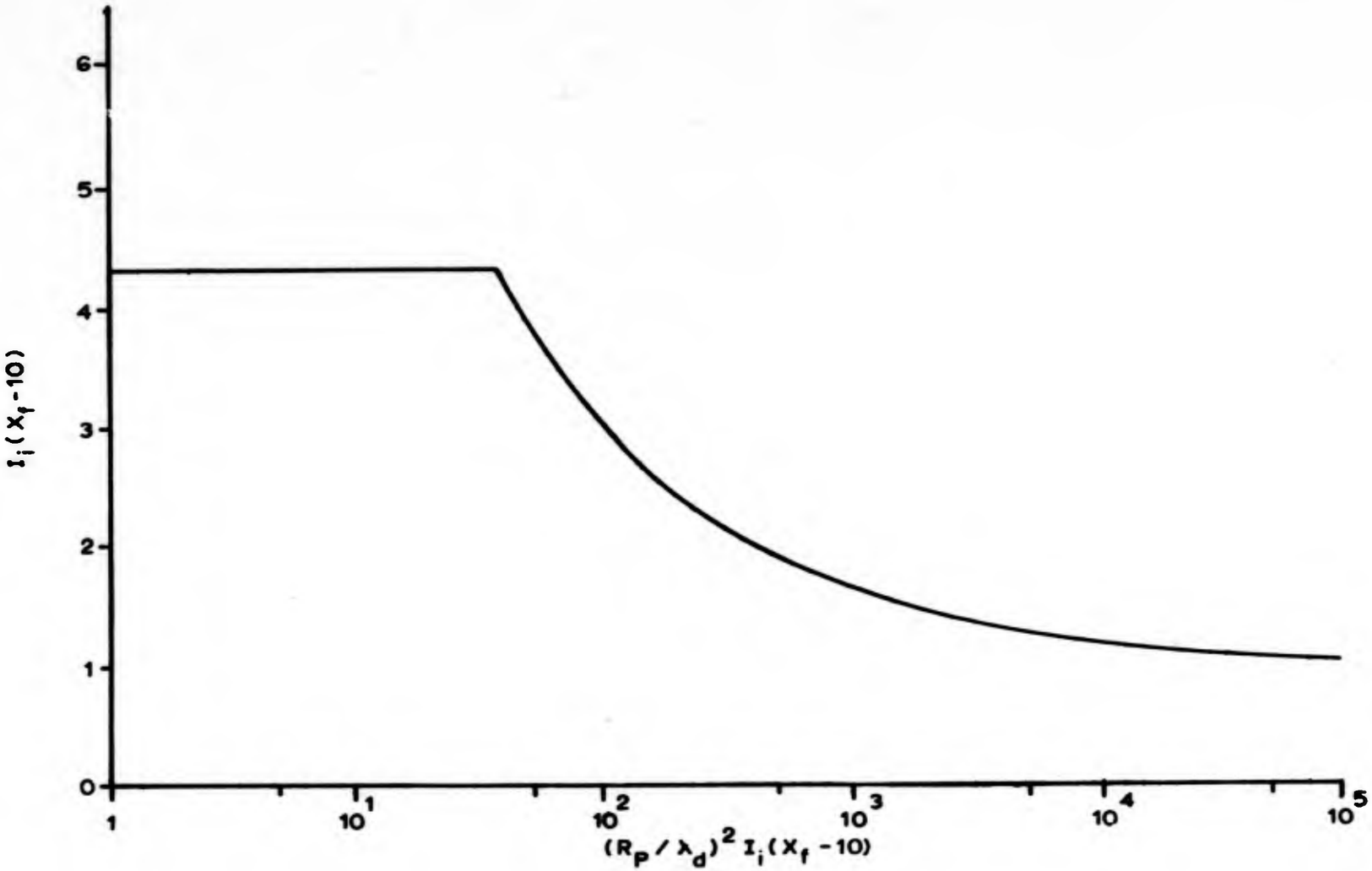

FIG. B-2

VARIATION OF $I_i(X_f-10)$ WITH $(R_P/\lambda_d)^2 I_i(X_f-10)$

(7) Calculate the ion number density in m^{-3} from

$$N_i = \frac{1.01 \times 10^{16}}{I_i(X_f - 10)} \times \frac{J_i(X_f - 10)}{(KT_e/e)^{\frac{1}{2}}} \qquad \text{(B-5)}$$

(8) Determine $j_e(0)$. This is done by drawing a tangent to the curve plotted in step 1 at a point $10(KT_e/e)$ above X_f. The value of j_e where this tangent intersects the slope tangent drawn in step 2 is $j_e(0)$.

(9) Calculate the electron number density in m^{-3} from

$$N_e = \frac{(4.02 \times 10^{12})\ j_e(0)}{(T_e)^{\frac{1}{2}}} \qquad \text{(B-6)}$$

where T_e is the electron temperature in degrees Kelvin calculated using Eq. (B-2).

In this project, a tungsten Langmuir probe was used having the dimensions:

diameter	0.0015 millimeter
langth	6.85 millimeter

The probe was cleaned by electron bombardment for one minute using 200 to 400 volts positive. This was followed by 15 seconds of ion bombardment using 50 volts negative. The Langmuir probe traces were taken using the x-y recorder listed in Appendix D. All traces were taken with the probe in the center of the plasma at the point where the electron gun beam passed through the plasma. When taken, the beam was not permitted past the first apperature. All calculations of number density and electron temperature were assumed to be averages across the interaction length.

It is important to realize that the procedure presented by Sonin uses the two tangent method for determining the plasma potential used

in the preceeding calculations. Although not shown directly, the plasma potential is the result obtained in step 8 which is used to calculate the electron number density. The two tangent method does not give very accurate results. The plasma potential thus obtained can in some cases be off by as much as 50 to 100 per cent. This can be shown by applying the more detailed second derivative technique to the probe trace. Thus, the electron number density calculations were questioned.

By carrying out numerical calculations, it was found that the ion number density changed very little as the probe current j_i was measured at points from $X_f - 10(KT_e/e)$ to $X_f - 20(KT_e/e)$. By using the same variation in step 8, the plasma potential and thus $j_e(0)$, was seen to vary noticeably. Using Eq. (B-5) and (B-6), it was concluded that the ion number density calculations were more reasonable.

Appendix C

Computer Program of Bethe's Solution

Symbols used:

B	is the solution of $B - \mathrm{Ln}\ B = f(\gamma_c/\gamma_a)$ for the known values of beam energy, plasma temperature and interaction distance
C	is the constant defined by Eq. (22)
CUR	is the ratio of the detector current to the input current (the input current is measured for a maximum angle θ of 10)
D	is the plasma number density (ion plus electron)
E	is the beam energy in ev
F(I,1)	is Moliere's series function f^0
F(I,2)	is Moliere's series function f^1
F(I,3)	is Moliere's series function f^2
FT	is the current detectable up to the angle θ
FTD	is the current measured by a detector cup having an apperature size θ_d
T	is the non-dimensional angle θ
TD	is the non-dimensional detector angle θ_d
XC	is the critical angle γ_c in radians

```
C  C  CALCULATION OF LIMITING THETA      LT MEURER
       T=2.0E-4
       B=12.76
       E=2000.0
       C=6.5131922E-13
     1 READ, D
       XC=SQRT(C*D)/E
       TD=T/(XC*SQRT(B))
       PUNCH,D,XC,TD
       GO TO 1
       STOP
       END
2.5E+8
1.0E+9
2.0E+9
4.0E+9
6.0E+9
8.0E+9
9.0E+9
1.6E+10
2.5E+10
4.0E+10
6.0E+10
1.0E+11
2.0E+11
4.0E+11
```

```
C  C  CALCULATION OF LIMITING THETA      LT MEURER
        N            Xc           θd
  2.5000E+08  8.5070E-06  6.5816
  1.0000E+09  1.7014E-05  3.2908
  2.0000E+09  2.4061E-05  2.3269
  4.0000E+09  3.4028E-05  1.6454
  6.0000E+09  4.1676E-05  1.3435
  8.0000E+09  4.8123E-05  1.1635
  9.0000E+09  5.1042E-05  1.0969
  1.6000E+10  6.8056E-05  8.2270E-01
  2.5000E+10  8.5070E-05  6.5816E-01
  4.0000E+10  1.0761E-04  5.2032E-01
  6.0000E+10  1.3179E-04  4.2484E-01
  1.0000E+11  1.7014E-04  3.2908E-01
  2.0000E+11  2.4061E-04  2.3269E-01
  4.0000E+11  3.4028E-04  1.6454E-01
```

NOTE: Knowing θ_d, the values of f^o, f^1 and f^2 can be found from Table I or from Figs. 2-5a and 2-5b. These values are then substituted into Bethe's table in the next program.

```
C  C  CALCULATION OF I/IO BY INTEGRATION        LT MEURER
      DIMENSION T(63),F(63,3)
      B=12.76
      E=1500.0
      DO 1 I=1,N
    1 READ,T(I),F(I,1),F(I,2),F(I,3)
    2 FT=0.0
      TA=0.0
      READ,D,XC,TD
      DO 5 I=1,N
      FB=(F(I,1)+F(I,2)/B+F(I,3)/B**2) (B*XC**2)
      FT=FT+(FB+FA)*(T(I)+TA)*(T(I)-TA)
      IF(T(I)-TD) 4,3,4
    3 FTD=FT
    4 TA=T(I)
    5 FA=FB
      CUR=FTD/FT
      PUNCH,D,FTD,FT,CUR
      GO TO 2
      STOP
      END
```

0.0	2.0	0.8456	2.4926
0.10494	1.99	0.79	2.31
0.14895	1.95	0.75	2.13
0.16454	1.95	0.74	2.11
0.15493	1.95	0.74	2.10
0.2	1.9212	0.7038	2.0694
0.21065	1.9	0.68	1.9
0.23269	1.89	0.67	1.89
0.29791	1.83	0.56	1.58
0.32908	1.8	0.5	1.42
0.33186	1.8	0.5	1.4
0.3846	1.75	0.385	1.16
0.4	1.7214	0.3437	1.0488
0.43484	1.7	0.3	0.95
0.47103	1.6	0.1	0.6
0.52032	1.54	0.0	0.38
0.52472	1.53	0.0	0.34
0.59581	1.41	-0.06	-0.0004
0.6	1.4094	-0.0777	-0.0044
0.65816	1.3	-0.168	-0.168
0.74477	1.12	-0.3	-0.45
0.8	1.0546	-0.3981	-0.6068
0.8227	1.0	-0.4	-0.61
0.99302	0.74	-0.52	-0.65
1.0	0.7338	-0.5285	-0.6359
1.0494	0.66	-0.52	-0.58
1.0533	0.66	-0.52	-0.58
1.0969	0.6	-0.505	-0.51
1.1635	0.52	-0.495	-0.385
1.2	0.4738	-0.4770	-0.3086
1.2162	0.45	-0.47	-0.29

1.3435	0.325	-0.38	0.0
1.3548	0.32	-0.375	0.0
1.4	0.2817	-0.3183	0.0535
1.4895	0.22	-0.23	0.15
1.6	0.1546	-0.1396	0.2423
1.6454	0.131	-0.094	0.258
1.8	0.0783	-0.0006	0.2386
2.0	0.0366	0.0782	0.1316
2.2	0.01581	0.1054	0.0196
2.3269	0.0092	0.105	-0.028
2.4	0.0063	0.1008	-0.0467
2.6	0.00232	0.08262	-0.0649
2.8	0.00079	0.06247	-0.0546
2.9791	0.000255	0.048	-0.036
3.0	0.00025	0.0455	-0.03568
3.2	0.000073	0.03288	-0.01923
3.2908	0.000039	0.028	-0.0125
3.3186	0.000034	0.0275	-0.0113
3.4	0.000019	0.02402	-0.00847
3.6	0.0000047	0.01791	-0.00264
3.8	0.0000011	0.01366	0.00005
4.0	0.0	0.010638	0.0010741
4.5	0.0	0.00614	0.0012294
5.0	0.0	0.003831	0.0008326
5.5	0.0	0.002527	0.0005368
5.9581	0.0	0.00175	0.00035
6.0	0.0	0.001739	0.0003495
6.5816	0.0	0.00117	0.000217
7.0	0.0	0.000908	0.0001584
8.0	0.0	0.0005211	0.0000783
9.0	0.0	0.0003208	0.0000417
10.0	0.0	0.0002084	0.0000237

2.5000E+08	8.5070E-06	6.5816
1.0000E+09	1.7014E-05	3.2908
2.0000E+09	2.4061E-05	2.3269
4.0000E+09	3.4028E-05	1.6454
6.0000E+09	4.1676E-05	1.3435
8.0000E+09	4.8123E-05	1.1635
9.0000E+09	5.1042E-05	1.0969
1.6000E+10	6.8056E-05	8.2270E-01
2.5000E+10	8.5070E-05	6.5816E-01
4.0000E+10	1.0761E-04	5.2032E-01
6.0000E+10	1.3179E-04	4.2484E-01
1.0000E+11	1.7014E-04	3.2908E-01
2.0000E+11	2.4061E-04	2.3269E-01
4.0000E+11	3.4028E-04	1.6454E-01

C C CALCULATION OF I/IO BY INTEGRATION LT MEURER

N	I	IO	I/IO
2.5000E+08	4.3372E+09	4.3421E+09	9.9886E-01
1.0000E+09	1.0762E+09	1.0855E+09	9.9142E-01
2.0000E+09	5.2883E+08	5.4279E+08	9.7429E-01
4.0000E+09	2.4522E+08	2.7138E+08	9.0358E-01
6.0000E+09	1.4707E+08	1.8092E+08	8.1288E-01
8.0000E+09	9.8722E+07	1.3569E+08	7.2755E-01
9.0000E+09	8.3061E+07	1.2061E+08	6.8865E-01
1.6000E+10	3.3443E+07	6.7846E+07	4.9293E-01
2.5000E+10	1.5528E+07	4.3421E+07	3.5762E-01
4.0000E+10	6.5983E+06	2.7136E+07	2.4316E-01
6.0000E+10	3.0801E+06	1.8092E+07	1.7024E-01
1.0000E+11	1.1487E+06	1.0855E+07	1.0582E-01
2.0000E+11	2.9585E+05	5.4279E+06	5.4506E-02
4.0000E+11	7.5203E+04	2.7138E+06	2.7711E-02

Appendix D

List of Major Equipment

1. X-Y Recorder, Mosely 2D-2.
2. Micro-microammeter, Keithly Model 410, PL 626B.
3. Electrometer, Keithley 600A, PL 554.
4. D.C. Power Supply (plasma), NJE Corporation Model HSV-5-20.
5. D.C. Power Supply (electron-gun), Power Design Pacific, Model HV-1556.
6. Pirani Vacuum Gauge, Consolidated Electrodynamics Corporation, Type GP 110, PL 443.
7. Ionization Gauge Meter, Consolidated Vacuum Corporation, Model GIO-110A, PL 451.
8. Electron Guns, Superior Electronics, Models SE-3M and SE-3W.
9. D.C. Power Supply (probe cleaning), Hewlett-Packard Model 712B.
10. D.C. Power Supply (probe bias), Kepco Model 25C-100-0.2, EMF 65.

GA/Phys/69-4

Vita

Earl L. Meurer was born on [redacted], the son of Earl Ruth and Virginia Fryer. After completing his secondary education at McAllen High School, McAllen, Texas, he legally changed his name prior to entering the University of Texas. He left school after two years and entered the Air Force. Upon completion of basic training, he was assigned to the electronics technical school at Keesler Air Force Base. After graduating, he remained there as a basic electronics instructor and earned his engineering associates degree in off duty schooling. He was then accepted for the Airman Education and Commissioning Program and received his degree of Bachelor of Aerospace Engineering at Auburn University in December, 1966. He was commissioned a Lieutenant in the Air Force after completing Officers Training School in March, 1967. Having been selected for a graduate program, he then came to the Air Force Institute of Technology in April, 1967.

Permanent Address: [redacted]

This thesis was typed by Mrs. Judith Ann Meurer

~~Unclassified~~
Security Classification

DOCUMENT CONTROL DATA - R&D

(Security classification of title, body of abstract and indexing annotation must be entered when the overall report is classified)

1. ORIGINATING ACTIVITY (Corporate author) Air Force Institute of Technology (AFIT-SE) Wright-Patterson AFB, Ohio 45433	2a. REPORT SECURITY CLASSIFICATION Unclassified 2b GROUP

3. REPORT TITLE

An Experimental Study of Moliere's Theory of Multiple Scattering

4. DESCRIPTIVE NOTES (Type of report and inclusive dates)

AFIT Thesis

5. AUTHOR(S) (Last name, first name, initial)

Earl L. Meurer
1/Lt. USAF

6. REPORT DATE	7a. TOTAL NO. OF PAGES	7b. NO. OF REFS
June 1969	86	16

8a. CONTRACT OR GRANT NO.	9a. ORIGINATOR'S REPORT NUMBER(S)
b. PROJECT NO. N/A	GA/Phys/69-4
c.	9b. OTHER REPORT NO(S) (Any other numbers that may be assigned this report)
d.	

10. AVAILABILITY/LIMITATION NOTICES This document is subject to special export controls and each transmittal to foreign governments or foreign nationals may be made only with prior approval of the Dean of Engineering, Air Force Institute of Technology (AFIT-SE), Wright-Patterson Air Force Base, Ohio 45433

11. SUPPLEMENTARY NOTES	12. SPONSORING MILITARY ACTIVITY

13. ABSTRACT

This study investigates the possible use of electron beam scattering techniques and Moliere's multiple scattering theory to infer plasma charged particle number densities. By modifying an existing small angle scattering device, experimental measurements of electron beam attenuation through a plasma were obtained. After correcting for neutral background heating effects, these values were then compared to values predicted by Moliere's theory. From this study, it was concluded that electron beam scattering techniques using Moliere's theory of multiple scattering could indeed be used to determine plasma charged particle number densities.

DD FORM 1 JAN 64 1473

Security Classification

14 KEY WORDS	LINK A		LINK B		LINK C	
	ROLE	WT	ROLE	WT	ROLE	WT
Electron Beam Scattering Weakly ionized plasma Plural Scattering Multiple Scattering Moliere's Theory of Multiple Scattering Neutral Heating Effect Determination of plasma number densities						

INSTRUCTIONS

1. ORIGINATING ACTIVITY: Enter the name and address of the contractor, subcontractor, grantee, Department of Defense activity or other organization *(corporate author)* issuing the report.

2a. REPORT SECURITY CLASSIFICATION: Enter the overall security classification of the report. Indicate whether "Restricted Data" is included. Marking is to be in accordance with appropriate security regulations.

2b. GROUP: Automatic downgrading is specified in DoD Directive 5200.10 and Armed Forces Industrial Manual. Enter the group number. Also, when applicable, show that optional markings have been used for Group 3 and Group 4 as authorized.

3. REPORT TITLE: Enter the complete report title in all capital letters. Titles in all cases should be unclassified. If a meaningful title cannot be selected without classification, show title classification in all capitals in parenthesis immediately following the title.

4. DESCRIPTIVE NOTES: If appropriate, enter the type of report, e.g., interim, progress, summary, annual, or final. Give the inclusive dates when a specific reporting period is covered.

5. AUTHOR(S): Enter the name(s) of author(s) as shown on or in the report. Enter last name, first name, middle initial. If military, show rank and branch of service. The name of the principal author is an absolute minimum requirement.

6. REPORT DATE: Enter the date of the report as day, month, year, or month, year. If more than one date appears on the report, use date of publication.

7a. TOTAL NUMBER OF PAGES: The total page count should follow normal pagination procedures, i.e., enter the number of pages containing information.

7b. NUMBER OF REFERENCES: Enter the total number of references cited in the report.

8a. CONTRACT OR GRANT NUMBER: If appropriate, enter the applicable number of the contract or grant under which the report was written.

8b, 8c, & 8d. PROJECT NUMBER: Enter the appropriate military department identification, such as project number, subproject number, system numbers, task number, etc.

9a. ORIGINATOR'S REPORT NUMBER(S): Enter the official report number by which the document will be identified and controlled by the originating activity. This number must be unique to this report.

9b. OTHER REPORT NUMBER(S): If the report has been assigned any other report numbers *(either by the originator or by the sponsor)*, also enter this number(s).

10. AVAILABILITY/LIMITATION NOTICES: Enter any limitations on further dissemination of the report, other than those imposed by security classification, using standard statements such as:

(1) "Qualified requesters may obtain copies of this report from DDC."

(2) "Foreign announcement and dissemination of this report by DDC is not authorized."

(3) "U. S. Government agencies may obtain copies of this report directly from DDC. Other qualified DDC users shall request through

_____."

(4) "U. S. military agencies may obtain copies of this report directly from DDC. Other qualified users shall request through

_____."

(5) "All distribution of this report is controlled. Qualified DDC users shall request through

_____."

If the report has been furnished to the Office of Technical Services, Department of Commerce, for sale to the public, indicate this fact and enter the price, if known.

11. SUPPLEMENTARY NOTES: Use for additional explanatory notes.

12. SPONSORING MILITARY ACTIVITY: Enter the name of the departmental project office or laboratory sponsoring *(paying for)* the research and development. Include address.

13. ABSTRACT: Enter an abstract giving a brief and factual summary of the document indicative of the report, even though it may also appear elsewhere in the body of the technical report. If additional space is required, a continuation sheet shall be attached.

It is highly desirable that the abstract of classified reports be unclassified. Each paragraph of the abstract shall end with an indication of the military security classification of the information in the paragraph, represented as *(TS), (S), (C), or (U)*.

There is no limitation on the length of the abstract. However, the suggested length is from 150 to 225 words.

14. KEY WORDS: Key words are technically meaningful terms or short phrases that characterize a report and may be used as index entries for cataloging the report. Key words must be selected so that no security classification is required. Identifiers, such as equipment model designation, trade name, military project code name, geographic location, may be used as key words but will be followed by an indication of technical context. The assignment of links, rules, and weights is optional.